NASA CR-175150

(NASA-CR-175150) EARTH STRAIN MEASUREMENTS WITH THE TRANSPORTABLE LASER RANGING SYSTEM: FIELD TECHNIQUES AND PLANNING Final Report, Dec. 1979 - Nov. 1982 (Texas Univ.) 42 p HC A03/MF A01 CSCL 08G G3/46 N84-17725 Unclas 12212

THE UNIVERSITY OF TEXAS AT AUSTIN
Institute For Geophysics

EARTH STRAIN MEASUREMENTS
WITH THE TRANSPORTABLE LASER RANGING SYSTEM:
FIELD TECHNIQUES AND PLANNING

Yosio Nakamura
H. James Dorman
Thomas Cahill

The University of Texas at Austin
Institute for Geophysics
Galveston Marine Geophysics Laboratory
700 The Strand
Galveston, Texas 77550-2768

November 1982
Final Report for Period December 1979 - November 1982
NASA Contract NAS5-25897

Prepared for
GODDARD SPACE FLIGHT CENTER
Greenbelt, Maryland 20771
Technical Officer: Christopher C. Stephanides, Code 942

The University of Texas Institute for Geophysics
Contribution No. 532

ABSTRACT

We have conducted a feasibility study to examine the potential of the Transportable Laser Ranging System (TLRS) for monitoring the ground deformation around satellite ranging stations and other geodetic control points. Emphasis has been placed on testing the usefulness of the relative lateration technique. The temporal variation of the ratio of the length of each survey line to the mean length of all survey lines in a given area is directly related to the mean shear strain rate for the area. The data from a series of experimental measurements taken over the Los Angeles basin from a TLRS station at Mt. Wilson show that such ratios can be determined to an accuracy of one part in 10^7 with a measurement program lasting for three days and without using any corrections for variations in atmospheric conditions. A numerical experiment using a set of hypothetical data indicates that reasonable estimates of the present shear strain rate and the direction of the principal axes in southern California can be deduced from such measurements over an interval of one to two years. Thus, the relative lateration from the TLRS appears to be a very economical way to monitor ground deformations, although there has been no opporunity yet to measure the actual ground strain by reoccupying the Mt. Wilson site.

Table of Contents

I. INTRODUCTION

With the recent development in ground-to-satellite laser ranging and Very Long Baseline Interferometry (VLBI) techniques, it is now possible to measure precisely distances between locations separated by several hundreds to thousands of kilometers. This makes it possible to monitor relative movements of globally distributed points on the earth for geodynamic studies. However, one question that must be answered is how representative each of these positions thus occupied is for the region in which it is located. If some of these locations are experiencing localized movements which are not representative of the region, the global measurement would give erroneous results. An answer to this questions can be found by measuring regional deformations around each location.

A conventional method for determining regional deformations is to perform repeated survey using an electro-optical distance measuring (EDM) device (e.g. Savage et al. [1981]). However, such surveys are expensive, and are rather limited in range. We, therefore, have looked for a better alternative. The development of the Transportable Laser Ranging System (TLRS) for ground-to-LAGEOS (Laser Geodynamics Earth Orbiting Satellite) ranging [Silverberg and Byrd, 1981] has given us an opportunity to test such an alternative. Because of its high sensitivity, being capable of detecting single photon returns, the TLRS can measure distances to small targets (retro-reflectors) at any visible points much beyond the normal ranges of other EDM devices. Thus, this system may provide economical measurements of strain fields in areas more than 200 km in diameter. If successful, such measurements will be valuable not only in the immediate neighborhood of satellite ranging stations, but also in understanding the dynamic behavior of both plate boundaries and areas internal to plates.

We have conducted a limited feasibility study to examine this potential. Although the TLRS is a powerful system, it also has certain limitations when used for a ground-to-ground ranging. The most important is the uncertainty of measurement results due to variability in atmospheric conditions. To bypass this problem and avoid the expense of flying an aircraft to monitor the atmospheric conditions along the path of the laser beam, we have examined the use of the relative lateration, or the ratio method, which was used earlier by Carter and Vincenty [1978] in an experimental survey around the McDonald Observatory.

We originally planned repeated field experiments at several sites in the western United States. However, because of many scheduling conflicts and delays associated with the overall TLRS-LAGEOS ranging experiments, the only field experiment we could perform during the current contract was a four-day measurement at Mt. Wilson over the Los Angeles basin in January, 1981. We have been unable to reoccupy this site for an actual strain measurement.

The present study, however, has given us some very encouraging results. Even with no atmospheric correction at all, the range ratios could be determined to an accuracy of one part in 10^7. This is sufficient for an order-of-magnitude estimate of incremental shear strain in the southern California region if two measurements separated by one to two years are available. Higher accuracies would be attainable with repeated measurements.

In this report, we first describe the advantages and problems of ground-to-ground ranging by a TLRS, leading to the use of relative lateration, or range-ratio method, and its relationship to the regional strain (Section II). Then, we present the data and analysis of the Mt. Wilson experiment (Section III). This is followed by a short treatment of regional strain determination using hypothetical data (Section IV). Finally, we present the conclusions from this feasibility study and offer some recommendations. Some pertinent data are presented in the Appendix.

II. TLRS GROUND-TO-GROUND RANGING

Advantanges and Problems

The TLRS is a highly mobile satellite laser ranging system designed to perform ground-to-LAGEOS range measurements. It is also highly sensitive, being capable of determining the range to a LAGEOS satellite with return signals as low as one photelectron every 20 to 50 laser shots [Silverberg et al. 1982]. Used as a ground-to-ground ranging device, it can measure the distance to any single 1 inch (25 mm) corner reflector within sight at very low laser power level. The measureable range is limited only by the curvature of the earth. The required power level is so low that, unlike some systems used for similar measurements, the laser beam can be maintained many orders of magnitude below the eye-damage threshold.

The practical precision of the TLRS range measurements is limited to about 1.5 cm for a one minute average, which is somewhat worse than those of conventional EDM devices using modulated laser beams. However, the long range capability of the TLRS reduces the relative error to well within the limits of interest in conventional surveys. The TLRS has an automatic pointing system, an automatic calibration system and other features which lend themselves to providing many horizontal (ground-to-ground) line measurements on an operational basis. Thus it will be a good device to use if the data it provides is sufficient to determine the regional deformation at a high-enough accuracy.

The most serious problem in using the TLRS for ground-to-ground ranging is the atmospheric effect. The temperature, pressure, and to a lesser degree water vapor influence the index of refraction of air, and thus the speed of a laser beam through the atmosphere. To obtain the absolute distance between two points from a time of flight measurement through air, one must make corrections for these atmospheric variables.

Estimates of these atmospheric variables along the beam path may be made based on measurements at the two end points. This, however, is unsatisfactory for long lines. A more precise way is to measure directly the atmospheric condition along the beam path by flying an aircraft during the ranging. This, though done in practice, is a costly operation. A third alternative is to use more than one wavelength for ranging. Using the dispersive characteristics of light in air, one can correct for the atmospheric effects [Huggett, et al. 1977].

The present TLRS operates in a single color. Flying an aircraft, we judged, is too costly for repeated measurements in many directions. Thus we had to look for another alternative.

Relative Lateration

One way to improve the accuracy of range measurements without relying on expensive in-flight measurement of atmospheric conditions is to use a relative lateration technique, or the "ratio method" (Robertson, 1972). Instead of attempting to measure the absolute length of each survey line to high accuracy, this technique determines only the ratios of distances. This method is based on a supposition that the temporal changes of atmospheric conditions along several survey lines within a given region are similar to each other. Therefore, even when the time of flight of a laser beam in each line fluctuates with changing atmospheric conditions, the ratios of the times of flight along different survey lines tend to vary little with time.

Carter and Vincenty [1978] used this method in an experimental EDM survey around the McDonald Observatory in 1977. They obtained sets of measurements, one month apart, consistent to one to two parts in 10^7. They have just repeated this experiment and the data is now being analyzed. Since the results of Carter and Vincenty appear to be quite promising, we have decided to try the same for our TLRS measurements.

Relationship Between Relative Lateration and Strain

Unlike absolute measurements of distances, the relative distance measurements repeated after a certain time period will not give all of the components of deformation, or incremental strain, for the time period unless at least one survey line is measured absolutely. However, a clear relationship exists between the changes of relative distances and incremental shear strain.

Let us consider n survey lines radiating from a central station. In the present case, the TLRS is located at the central station and a retroreflector is located at the end of each radiating line. Assume that all lines lie in a horizontal plane, neglecting both the curvature of the earth's surface and topographic height differences. Choosing a coordinate system with the origin at the central station, positive x towards east and positive y towards north, the original length of line i to the reflector at coordinates (x_i, y_i) at the time of the initial survey is given by

$$s_i = (x_i^2 + y_i^2)^{\frac{1}{2}} \tag{1}$$

Now assume that between the initial survey and a subsequent survey the entire area of the survey undergoes a uniform deformation represented by incremental strain components ε_{xx}, ε_{xy} and ε_{yy}. Then, the line length becomes

$$s_i' = [(x_i + \varepsilon_{xx}x_i + \varepsilon_{xy}y_i)^2 + (y_i + \varepsilon_{xy}x_i + \varepsilon_{yy}y_i)^2]^{1/2}$$

$$= [x_i^2 + y_i^2 + 2\varepsilon_{xx}x_i^2 + 4\varepsilon_{xy}x_iy_i + 2\varepsilon_{yy}y_i^2]^{1/2}$$

$$= s_i[1 + 2\varepsilon_{xx}\sin^2\alpha_i + 4\varepsilon_{xy}\sin\alpha_i\cos\alpha_i + 2\varepsilon_{yy}\cos^2\alpha_i]^{1/2}$$

$$= s_i[1 + \varepsilon_{xx}\sin^2\alpha_i + \varepsilon_{xy}\sin 2\alpha_i + \varepsilon_{yy}\cos^2\alpha_i] \quad (2)$$

where $\alpha_i = \tan^{-1}(x_i/y_i)$ is the azimuth of the line i measured clockwise from north, and the higher order terms in strain have been neglected. Then, the range increment δ_i is given by

$$\delta_i = s_i' - s_i = s_i[\varepsilon_{xx}\sin^2\alpha_i + \varepsilon_{xy}\sin 2\alpha_i + \varepsilon_{yy}\cos^2\alpha_i] \quad (3)$$

Next define original mean range and range ratios to the mean, respective, as

$$\bar{s} = \sum_{i=1}^{n} s_i/n \quad (4)$$

and

$$r_i = s_i/\bar{s} \quad (5)$$

Then, the subsequent mean range and range ratios are

$$\bar{s}' = \sum_{i=1}^{n} s_i'/n = \bar{s} + \sum_{i=1}^{n} \delta_i/n \quad (6)$$

and

$$r_i' = s_i'/\bar{s}' = (s_i + \delta_i)/(\bar{s} + \sum_{i=1}^{n} \delta_i/n)$$

$$= r_i(1 + \delta_i/s_i - \sum_{i=1}^{n} \delta_i/n\bar{s}) \quad (7)$$

where the higher order terms are again neglected. The increment of the range ratio is, therefore,

$$r_i' - r_i = r_i(\delta_i/s_i - \sum_{i=1}^{n} \delta_i/n\bar{s}) \quad . (8)$$

Then, range ratio increment normalized by the original range ratio is given by

$$\gamma_i = (r_i' - r_i)/r_i = \delta_i/s_i - \sum_{i=1}^{n} \delta_i/n\bar{s} \tag{9}$$

Substituting eq. (3) into eq. (9), and using (5), we obtain

$$\begin{aligned}\gamma_i = {} & [\sin^2\alpha_i - \sum_{i=1}^{n}(r_i\sin^2\alpha_i)/n]\ \varepsilon_{yy} \\ & + [\sin 2\alpha_i - \sum_{i=1}^{n}(r_i\sin 2\alpha_i)/n]\ \varepsilon_{xy} \\ & + [\cos^2\alpha_i - \sum_{i=1}^{n}(r_i\cos^2\alpha_i)/n]\ \varepsilon_{yy}\end{aligned} \tag{10}$$

Equation (10) may give one an impression that a set of measurements of the normalized range ratio increments γ_i would give the incremental strain components ε_{xx}, ε_{xy} and ε_{yy}. However, this impression is incorrect because the coefficients of ε_{xx} and ε_{yy} are not independent of each other, as their sum vanishes, and therefore ε_{xx} and ε_{yy} cannot be determined uniquely.

Now let

$$\Theta = \varepsilon_{xx} + \varepsilon_{yy} \tag{11}$$

and

$$\Psi = \varepsilon_{xx} - \varepsilon_{yy} \tag{12}$$

Then,

$$\varepsilon_{xx} = \tfrac{1}{2}\ (\Theta + \Psi) \tag{13}$$

and

$$\varepsilon_{yy} = \tfrac{1}{2}\ (\Theta - \Psi) \tag{14}$$

Substituting (13) and (14) into (10), we obtain

$$\begin{aligned}\gamma_i = {} & [\sin\ 2\alpha_i - \sum_{i=1}^{n}(r_i\sin\ 2\alpha_i)/n]\ \varepsilon_{xy} \\ & - \tfrac{1}{2}\ [\cos\ 2\alpha_i - \sum_{i=1}^{n}(r_i\cos\ 2\alpha_i)/n]\ \Psi\end{aligned} \tag{15}$$

The coefficients of ε_{xy} and Ψ are known quantities for the initial setup of the survey lines. Thus, for a set of measurements of the normalized range ratio increments γ_i, the incremental shear strain components ε_{xy} and Ψ can be determined by a least-square inversion of eq. (15).

Finally, the maximum incremental shear strain S and the direction of the principal strain axes β are given by

$$S = [(2\varepsilon_{xy})^2 + \Psi^2]^{\frac{1}{2}} \tag{16}$$

and

$$\beta = \tfrac{1}{2}\tan^{-1}(2\varepsilon_{xy}/\Psi) \tag{17}$$

The dilation Θ of eq. (11) disappears from eq. (15), and thus cannot be determined. This is expected because any uniform compression or expansion of the entire area causes no change in range ratios.

The treatment above assumes uniform deformation of the entire region. If for some reason, such as the existence of active faults within the area, the regional deformation is not uniform, large residuals will show up in the least-square inversion of eq. (15). Thus, any residuals significantly larger than the measurement errors will indicate heterogeneous strain.

The remaining question is how accurately we can estimate the normalized range ratio increments γ_i. Since the measurements are done in terms of time of flight of light beams, the uncertainty in speed of light is the determining factor. The average speed of light, c_i, between the central station and a reflector i may be expressed as the sum of four components:

$$c_i = c_o + \ell_i + w_c + w_i \tag{18}$$

where c_o is the speed of light in standard air, which is constant for all survey lines at all times; ℓ_i is the correction attributable to the reflector location, which is time invariant for a given reflector; w_c is a component of correction attributable to weather common to all reflectors at a given time; and w_i is the residual weather correction. The line length s_i is given in terms of round-trip time of flight, t_i, as

$$s_i = \tfrac{1}{2}(c_o + \ell_i + w_c + w_i)t_i \tag{19}$$

the mean range as

$$\bar{s} = \tfrac{1}{2}(c_o\bar{t} + \sum_{i=1}^{n} \ell_i t_i/n + w_c\bar{t} + \sum_{i=1}^{n} w_i t_i/n) \tag{20}$$

where $\bar{t} = \sum_{i=1}^{n} t_i/n$ is the mean time of flight, and the range ratio to the mean as

$$r_i = u_i[1 + (\ell_i - \sum_{i=1}^{n} \ell_i t_i/n\bar{t} + w_i - \sum_{i=1}^{n} w_i t_i/n\bar{t})/c_o] \tag{21}$$

where $u_i = t_i/\bar{t}$ is the time-of-flight ratio to the mean, and the higher-order terms have been neglected. Finally, the normalized range ratio increment is given as

$$\gamma_i = \eta_i + [(w_i' - w_i) - \sum_{i=1}^{n} (w_i' - w_i)t_i/n\bar{t}]/c_o \tag{22}$$

where $\eta_i = (u_i' - u_i)/u_i$ is the normalized time-of-flight ratio increment and quantities with primes designate those at subsequent measurement as before. The higher-order terms are again neglected. Note that the common weather component, w_c, is eliminated by taking the range ratio (21), and the location specific components, ℓ_i's, are eliminated by normalization (22), leaving only the residual weather components w_i's.

The normalized time-of-flight ratio increment, η_i, thus approximates the range ratio increments, γ_i, with a small error due to residual weather term. The latter is not location specific, and is not common to all lines at a given time. If this term is sufficiently small, then we can substitute η_i for γ_i in calculating the shear strain increment using (15).

III. MT. WILSON EXPERIMENT

Field Experiment

At the request of the NASA Crustal Dynamics Project, the TLRS team from the McDonald Observatory of the University of Texas, led by Dr. Eric Silverberg, deployed the TLRS at Mt. Wilson, California, in January of 1981. At the same time, two of us (H.J.D. and T.C.) scouted the surrounding area for suitable target sites and selected the reflector locations. Then, a field party from the National Geodetic Survey (NGS), which was dispatched at the request of NASA to help us, deployed retroreflectors at the chosen sites. The survey lines selected for the site are shown in Figure 1. Table 1 lists the nominal coordinates of the base station (TLRS site) at Mt. Wilson and of the end points of the lines, where the retroreflectors were installed. Also listed in Table 1 are the approximate look angles from Mt. Wilson and ranges as computed from the indicated coordinates using the IAG standard ellipsoid Geodetic Reference System 1967.

Each reflector except the one at Cahuenga was a metal box containing an array of three 1½ inch (38mm) corner cubes, supplied by the NGS. The box was mounted on a tripod and placed directly over the station mark using an optical blumb bob. This elaborate configuration made it necessary to guard the reflector continuously for the entire duration of the experiment. The reflector used at Cahuenga was designed by one of us (T.C.) for unmanned operation. It contained a single 1 inch (25mm) corner cube and was fastened to an outcrop with anchor bolts at a site off the station mark, thus concealed from public view.

The reference point of the TLRS, from which the raw time-of-flight measurements were made, was slightly offset from the Mt. Wilson station mark given in Table 1. The measured coordinates of the station mark relative to the TLRS were:

$$x = -1.4873 \text{ m (west)}$$

$$y = 0.5093 \text{ m (north)}$$

$$z = -3.3709 \text{ m (below)}$$

The resulting corrections, to be applied to the observed quantities to reduce them to the reference mark, are listed in Table 2. The corrections can be applied at any stage of data reduction.

After the initial setup, which began on January 9, 1981, the horizontal ranging data were collected over the four-day interval January 23 through 26, 1981, in cooperation with the NOAA National Geodetic Survey. Each of the reflector sites except Cahuenga was manned continuously during the entire experiment to record the temperature, pressure and relative humidity at the site at about 30 minute intervals. The details of the data acquisition are given in Silverberg _et al._ [1982].

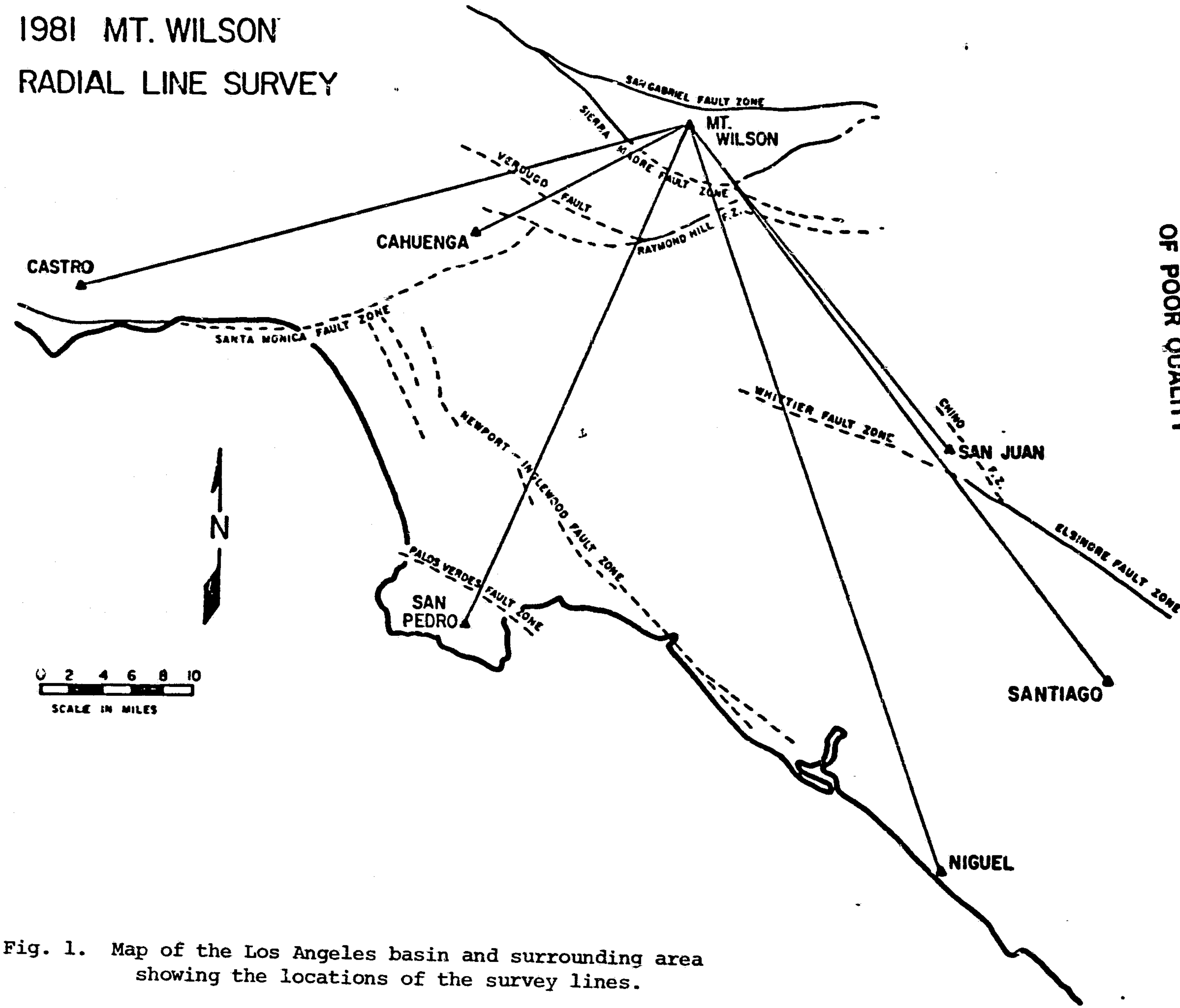

Fig. 1. Map of the Los Angeles basin and surrounding area showing the locations of the survey lines.

Table 1. Stations Used in Mt. Wilson Line Survey

Station	Longitude	Latitude	Elevation m	Look Angle Azimuth	Look Angle Altitude	Range m	Note
Mt. Wilson	241° 56' 17.85"	34° 13' 21.58"	1722.0				1
Castro	241° 12' 55.40"	34° 05' 08.57"	858.9	257.366	-1.030	68393	2
Cahuenga	241° 40' 29.81"	34° 08' 13.00"	554.1	248.687	-2.681	26104	3
San Pedro	241° 39' 55.73"	33° 44' 40.88"	447.1	205.506	-1.508	58729	4
Niguel	242° 16' 00.18"	33° 30' 44.83"	288.0	158.814	-1.353	84459	
Santiago	242° 28' 00.10"	33° 42' 37.89"	1733.0	139.168	-0.329	74933	
San Juan	242° 15' 45.99"	33° 54' 49.47"	543.0	138.751	-1.688	45536	

1 New marker 9.408m from Mt. Wilson E10A @345° 17'
2 Solitice Canyon B2 Aux. 1, which is 14.107m ENE of Castro 1898
3 Reference mark #3 of Cahuenga #2, 13.329m @257° 47' from Cahuenga #2
4 L7 Ecc. San Pedro Hills, which is 12.576m @318° 57' from San Pedro #3

Table 2. Corrections to be Applied to Observations to Reduce to Mt. Wilson Gound Marker

Station	Round-Trip Time of Flight ns	Range m	Range Ratio* (1) ppm	Range Ratio* (2) ppm
Castro	-9.344	-1.4003	-25.08	-26.78
Cahuenga	-9.054	-1.3568	-23.35	-23.51
San Pedro	-1.798	-0.2694	-5.91	-7.93
Niguel	6.222	0.9325	13.61	9.93
Santiago	8.931	1.3385	20.64	17.07
San Juan	8.432	1.2636	20.09	17.64

* (1) Ratio to mean range
(2) Same but excluding Cahuenga and Niguel

The Data

The raw field data were initially processed at the University of Texas at Austin by the McDonald Observatory group. As described in detail by Silverberg et al. [1982], the processing of the raw data involved accumulation of individual photon returns into 200 psec bins, smoothing of the coadded returns by three-bin (600 psec) running averages, cross-corretation with a reference standard to eliminate long-term drift in the calibration constants, adjustments to account for certain measurement irregularities, and removal of a 86.8 nsec constant calibration correction.

The calibrated round-trip time-of-flight data, shown in Figure 2 and listed in Table A1 in the Appendix, have not been corrected for the offset of the TLRS from the ground marker (Table 2). The data for Cahuenga were not used for the analysis because of certain processing difficulties encountered for the data for this station.

The data gap during the second day of observation was due to an interruption in data acquisition caused by rain which accompanied the passage of a cold front. The meteorological data taken at Mt. Wilson site and other stations are shown in Figures A1 through A3, and are listed in Table A2 in the Appendix.

As expected, the raw time-of-flight data show large fluctuations, which are only partially correlated with the meteorological data. The relative RMS deviations of the time-of-flight data (Table 3, column 3) range from 1.53 ppm for Niguel, which was surveyed only after the passage of the cold front, to 3.78 ppm for San Juan, which was the shortest line. The weighted average for all lines is 2.84 ppm.

Range Ratios to a Single Reference Line

Silverberg et al. [1982] calculated the time-of-flight ratios and atmosphere-corrected range ratios to a reference line following the procedure used by Carter and Vincenty [1978]. The reference line they chose was a smoothed curve (a cubic spline) through the Santiago data. Their results (Table 3, column 5) show relative RMS deviations of time-of-flight ratios ranging from 0.4 ppm for Niguel to 1.6 ppm for San Juan. The weighted average for all lines is 1.0 ppm, which is about a factor of three improvement from the fluctuation of the time-of-flight data.

Their results for the range ratios with atmospheric corrections based on end-point meteorological data did not fare as well. In fact the relative RMS deviations increased typically about 40% from those of uncorrected time-of-flight ratios [Silverberg et al. 1982].

ORIGINAL PAGE IS
OF POOR QUALITY

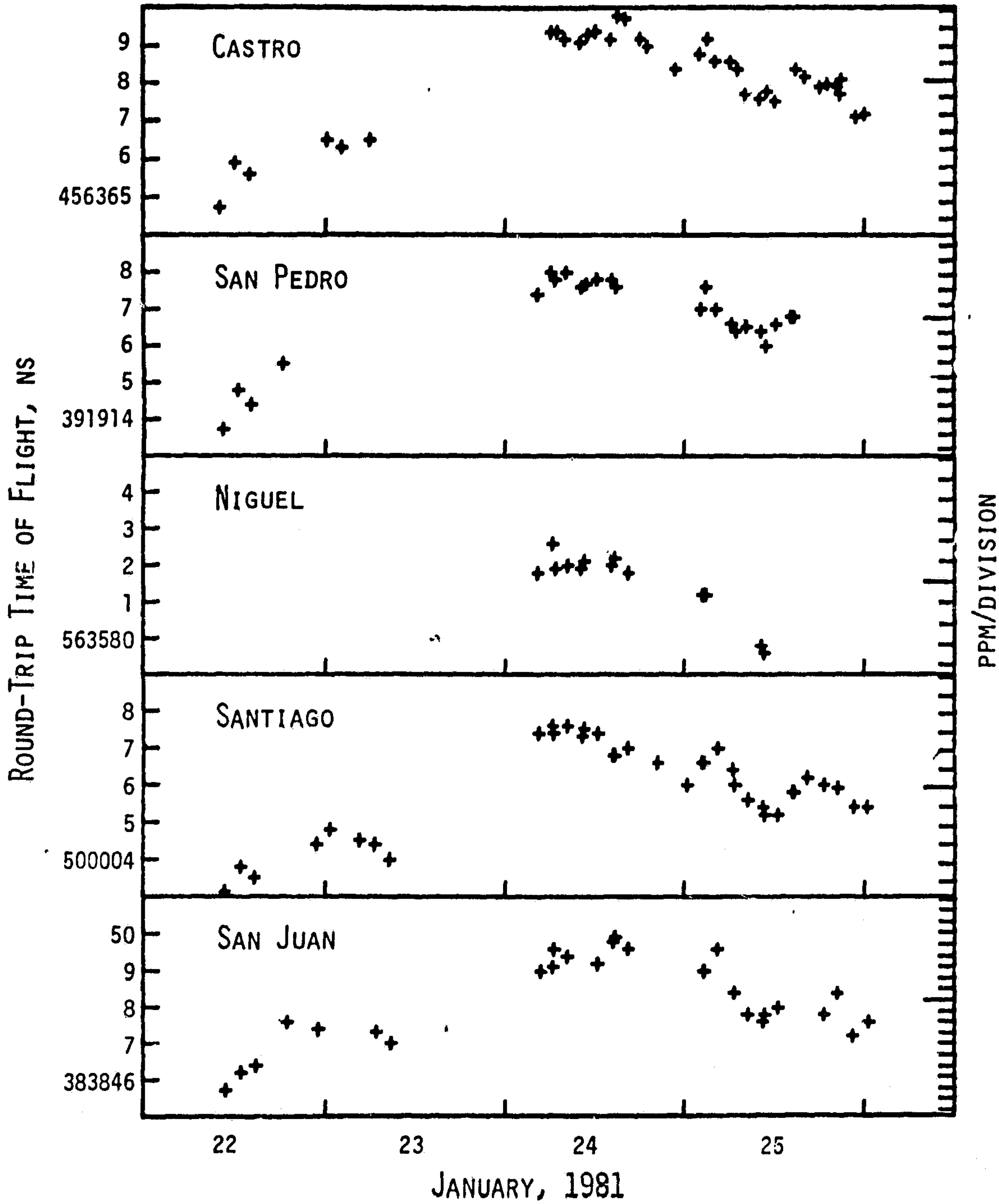

Fig. 2. Round-trip time of flight from Mt. Wilson. The data are not corrected for the marker offset.

The main reason for the poor performance of atmosphere-corrected values is the difficulty of making proper atmospheric corrections. A comparison of the variations of the group index of refraction calculated from the temperature and pressure at end points (Figure 3; also listed in Table A3 in the Appendix) with the time-of-flight variations (Figure 2) clearly shows that long-term variations are fairly well matched but shorter diurnal fluctuations are larger for the index of refractions than for the times-of-flight. Thus the index-of-refraction correction per Carter and Vincenty [1978] over-compensates for diurnal variations.

Time-of-Flight Ratios to the Mean

In order to be consistent with the range-ratio/strain relationship of the preceding section, we calculated the time-of-flight ratios to the mean. Since the time-of-flight measurements to all targets were not made exactly simultaneously, the data were linearly interpolated before the mean time-of-flight for a given time was calculated. (Higher order interpolations or a spline approximation might be better, but we judged the difference would be small.) Also, since we had data for Niguel only during the last half of the experiment, this station was excluded from the mean time-of-flight calculation.

The resulting time-of-flight ratios to the mean (Figure 4; also listed in Table A4 in the Appendix) show a further improvement in the fluctuations of the results. The relative RMS deviations (Table 3, column 5) now range from 0.36 ppm for Niguel to 1.24 ppm for San Juan, with the weighted average of 0.71 ppm for all lines, a factor of four improvement from the raw time-of-flight data.

An Alternative Atmospheric Correction

As stated earlier, the short-term, diurnal fluctuations in the index of refraction at end points exceed the observed fluctuations in the time-of-flight values. This is probably due to the larger fluctuation of the atmospheric temperature near the ground than those in most of the intervening air mass; a result of the base station and most of the target stations being located well above the intervening terrain. In this situation, a standard correction procedure like that of Carter and Vincenty [1978] is not really applicable, and some alternate procedures are needed.

An experimental procedure we tried was to estimate the average temperature of the air mass by low-pass filtering the mean of the temperatures measured at the end points. The filter we used was a simple one of adding all previous temperature readings each weighted by a factor proportional to a negative exponential of the elapsed time. After

ORIGINAL PAGE IS
OF POOR QUALITY

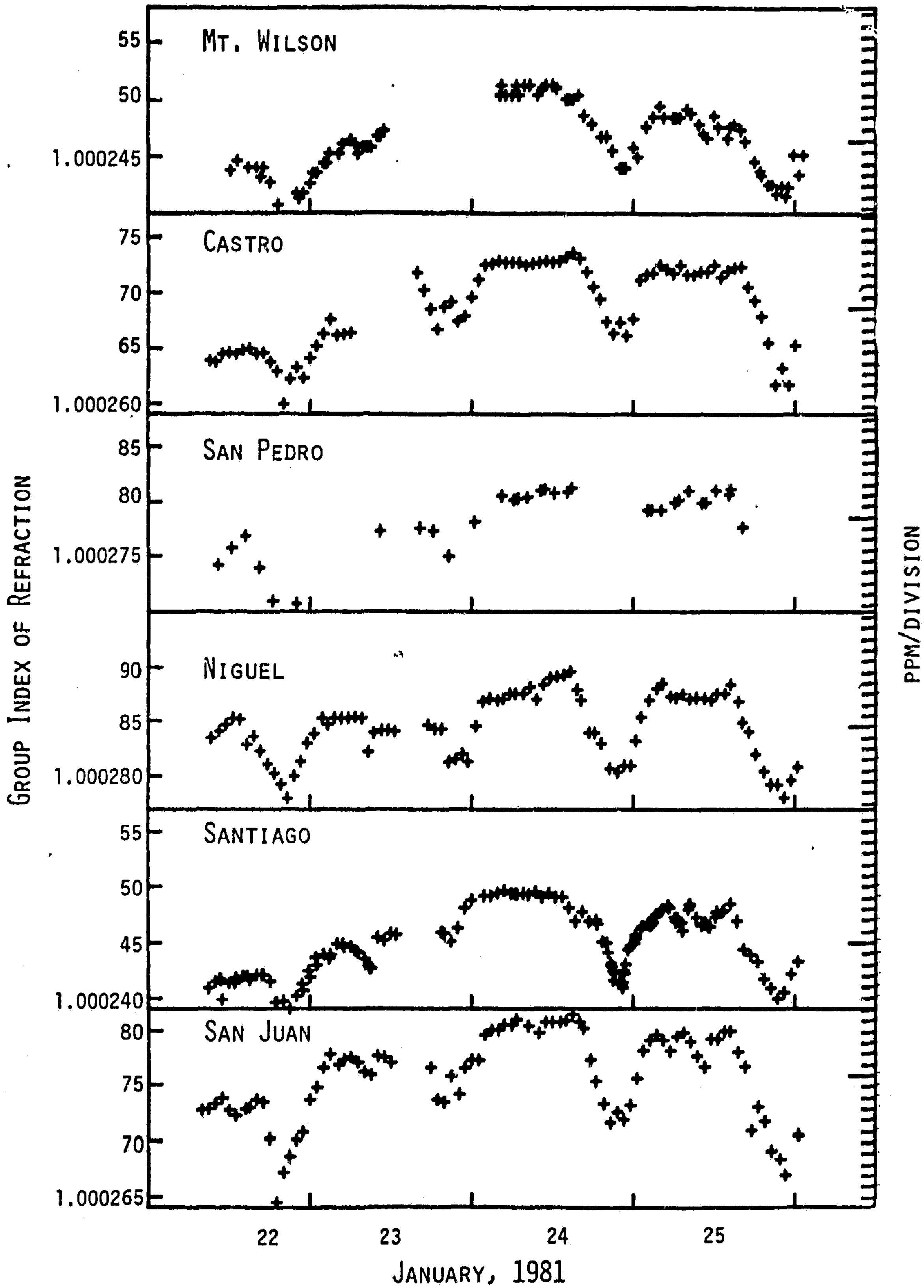

Fgi. 3. Group index of refraction computed from atmospheric data at end points.

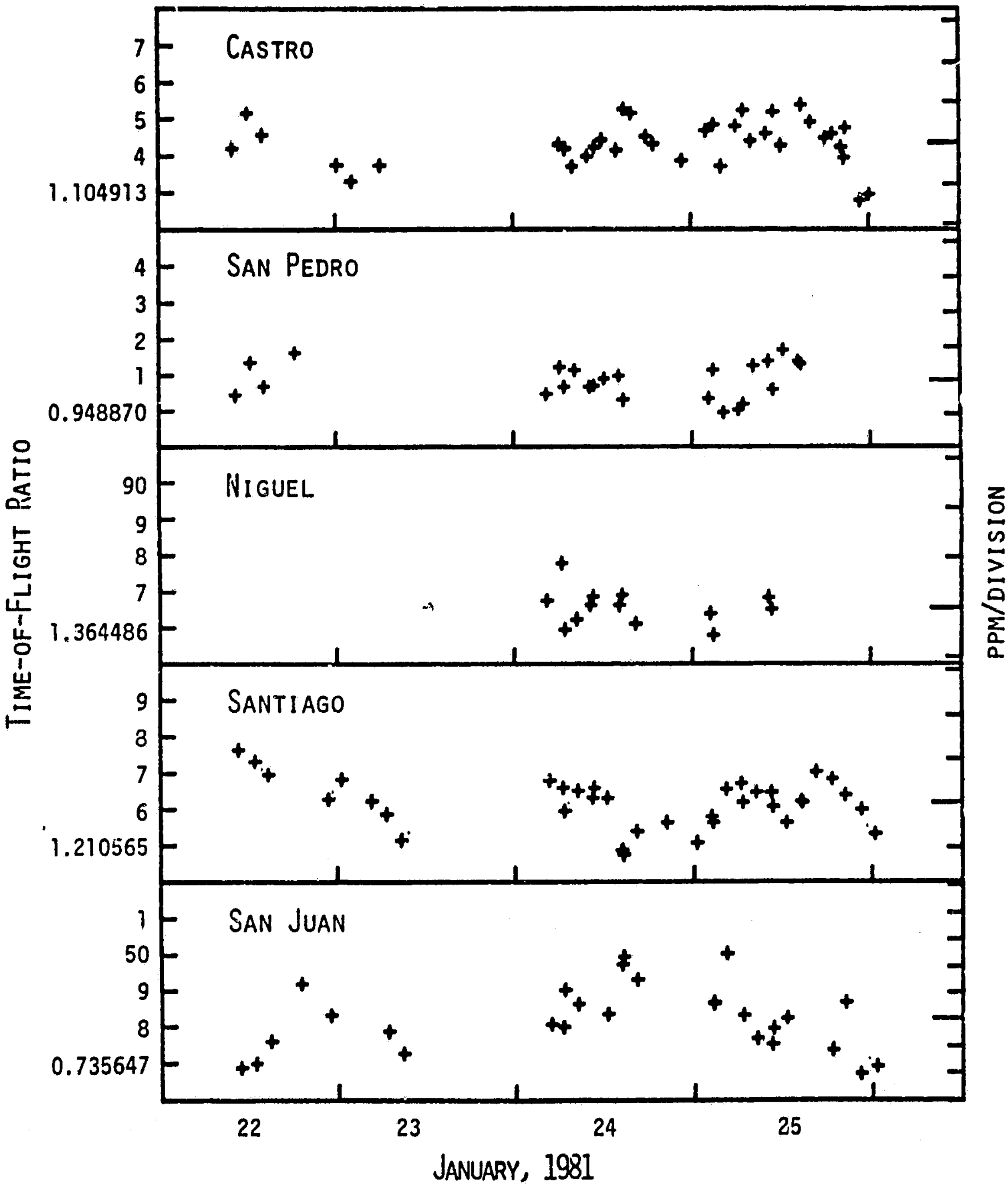

Fig. 4. Time-of-flight ratios to the mean.

trials with such filters of several different time constants, a time constant of 12 hours was found to give the best result. The resulting relative RMS deviations of the ranges thus corrected for atmospheric conditions (Table 3, column 4) range from 0.96 ppm for Castro to 2.05 ppm for San Juan with the weighted average of 1.38 ppm for all lines. This is about a factor of two improvement from the raw time-of-flight data. However, the range ratios calculated from these corrected ranges do not show any significant improvement over those of the uncorrected ratios. The relative RMS deviations of the corrected range ratios (Table 3, last column) range from 0.52 ppm for Niguel and Santiago to 1.21 ppm for San Juan, with the weighted average of 0.72 ppm for all lines.

A comparison of the relative RMS deviations of various quantities in Table 3 reveals that the best result is obtained for the uncorrected time-of-flight ratios to the mean. The atmospheric corrections did not improve the RMS deviations at all when ratios were taken.

A Test for Systematic Error Due to Atmospheric Conditions

The reliability of the relative lateration depends on the validity of the assumption that the temporal changes of atmospheric conditions are similar for all survey lines in the area so that their effects cancel out when ratios are taken. If this assumption is incorrect, a systematic error due to varying atmospheric conditions is introduced into the measured time-of-flight ratios. The greatly different atmospheric conditions before and after the passage of a cold front during the experiment gave us an opportunity to test this assumption.

The test we performed is the likelihood ratio test. We divided the time-of-flight ratios of Table A4 for each line into two subsets, the first half and the last half, of equal size (the last half was one greater than the first half if the total number was odd). If the systematic error due to atmospheric conditions is significantly large, the mean ratio, μ_1 , for the first subset will be significantly different from that, μ_2, for the second subset. Setting up a null hypothesis $H_o: \mu_1 = \mu_2$, if it is true, then the likelihood ratio statistic

$$t = [n_1 n_2/(n_1+n_2)]^{\frac{1}{2}} (\mu_1 - \mu_2)/[(n_1\sigma_1^2 + n_2\sigma_2^2)/(n_1+n_2 - 2)]^{\frac{1}{2}} \quad (23)$$

has a t distribution with n_1+n_2 -2 degrees of freedom, where n_1 and n_2 are the sample sizes of the two subsets and μ_1, μ_2 , σ_1^2 and σ_2^2 are used to designate the sample means and the sample variances of the first and the second subsets, respectively, for convenience.

At 90% significance level, the t distribution has values of 1.69 for 34 degrees of freedom and 1.80 for 11 degrees of freedom, while the t values computed from the data, Table 4, are much smaller. Therefore, the null hypothesis cannot be rejected at this level of significance.

ORIGINAL PAGE IS
OF POOR QUALITY

Table 3. Comparison of Relative RMS Deviations in ppm

Station	Number of Data Points	Uncorrected Time of Flight	Corrected Range(a)	Uncorrected T-o-F Ratio to Santiago(b)	Uncorrected T-o-F Ratio to the mean	Corrected Range Ratio to the mean
Castro	36	2.68	0.96	0.7	0.56	0.54
San Pedro	24	2.91	1.12	0.8	0.52	0.54
Niguel	13	1.53	1.81	0.4	0.36	0.52
Santiago	36	2.45	1.03	(0.2)	0.54	0.52
San Juan	27	3.78	2.05	1.6	1.24	1.21
All	136	2.84	1.38	1.0	0.71	0.72

(a) Corrected by using 12-hour low-pass filtered temperature
(b) From Silverberg et al. [1982]. The deviation for Santiago is from the smoothed curve, and is not included in calculating the average for all stations.

Table 4. Likelihood Ratio Test for Non-equality of Means

Station	Subset 1			Subset 2			Degree of Freedom	t
	n_1	μ_1	σ_1	n_2	μ_2	σ_2		
Castro	18	1.104914282	0.000000513	18	1.104914438	0.000000694	34	0.745
San Pedro	12	0.948870911	0.000000356	12	0.948870818	0.000000598	22	0.445
Niguel	6	1.364486713	0.000000572	7	1.364486460	0.000000365	11	0.889
Santiago	18	1.210566249	0.000000774	18	1.210566130	0.000000515	34	0.531
San Juan	13	0.735648159	0.000000830	14	0.735648288	0.000000983	25	0.353

In other words, no significant difference is found between the mean time-of-flight ratios in the first and second halves of the experiment for any of the lines surveyed.

Results

Since there is no evidence for systematic errors caused by atmospheric conditions, the most likely estimates of the mean time-of-flight ratios and their variances (and standard deviations) can be calculated from the entire data set. The results are shown in Table 5. Also listed in this table are the mean time-of-flight and the mean distances. The latter were calculated using atmospheric corrections based on the low-pass filtered temperatures described earlier and pressures interpolated to the average height of the beam from the end-point measurements (extrapolation in case of Santiago because the average height of the beam was lower than either end point). A group index of refraction of n_g=1.00028975 at the wavelength of 0.5320 μm, calculated from the formula given in American Institute of Physics Handbook [1972, p. 6-111] for standard dry air with 0.03% carbon dioxide at 15°C and 760 mm Hg, is used. No other corrections have been applied to the calculated distances; thus they are subject to minor systematic errors.

The estimated relative standard deviations of the mean time-of-flight ratios are approximately 1×10^{-7} except for San Juan, which is the shortest line. In comparison, Savage and Prescott [1973] estimate that the standard deviation of their Geodolite measurements of distances are 3 and 8 mm for lengths of 1 and 37 km, respectively. Thus, the precision of the present time-of-flight ratios is at least a factor of two better than that of their distance measurements. Furthermore, their distances had to be corrected for temperature and humidity readings made with an aircraft flying along the line of sight, while the present time-of-flight ratios required no atmospheric correction at all.

Multiwavelength measurements of distances are definitely better than the above two in terms of relative accuracy. Huggett and Slater [1975] and Slater and Huggett [1976] show the standard deviation of individual distance measurements to be less than 1×10^{-7} on a 10.1 km line. By taking the mean of many measurements, which is practical in this case, the accuracy can be improved further. The ranges attainable with the multiwavelength system, however, are quite limited compared with the TLRS measurements.

Table 5. Mean Time of Flight, Distance and Ratios*

Station	Mean Time of Flight ns	Mean Distance m	Mean T-o-F Ratio	S.D. of Mean T-o-F Ratio	Relative S.D. ppm
Castro	456358.75	68388.52	1.10488758	0.00000010	0.09
San Pedro	391914.94	58730.88	0.94886293	0.00000010	0.11
Niguel	563587.77	84456.72	1.36449651	0.00000014	0.10
Santiago	500014.83	74931.62	1.21058326	0.00000011	0.09
San Juan	303856.63	45535.87	0.73566587	0.00000018	0.24

* These results have been corrected for the TLRS/ground-marker offset.

Table 6. Increment in Normalized Ratio Due to Hypothetical Strain Increment and Rounded Values for Testing

Station	Normalized Ratio Increment ppm	Rounded to 0.1 ppm
Castro	0.052	0.1
San Pedro	-0.158	-0.2
Niguel	-0.030	0.0
Santiago	0.068	0.1
San Juan	0.070	0.1

IV. SHEAR STRAIN DETERMINATION USING HYPOTHETICAL DATA

We have been unable to reoccupy the Mt. Wilson site for a repeat measurement, which would allow a testing of the ratio method for a shear strain determination in the region. This section, therefore, describes an exercise we have conducted to see how well we can determine the regional shear-strain increment using a set of hypothetical data.

We assume a hypothetical strain increment described by

$\varepsilon_1 = 0.1 \times 10^{-6}$	:	maximum extension
$\varepsilon_2 = -0.2 \times 10^{-6}$	:	maximum compression
$\varepsilon_1 - \varepsilon_2 = 0.3 \times 10^{-6}$	:	maximum shear
$\beta = 110^\circ$	:	azimuth of maximum positive principal axis (extension) measured clockwise from north

This strain increment is approximately the annual strain increment in southern California observed by Savage et al. [1981]. The resulting increments in normalized range ratios for the five survey lines used in the Mt. Wilson experiment are listed in the center column of Table 6. Since we will not be able to measure these ratio increments at this accuracy, we use the values rounded to 1×10^{-7}, as given in the rightmost column of Table 6.

Substituting these rounded ratio increments into eq. (15), and inverting it in a least-squares sense, we obtain the following results:

$$\varepsilon_1 - \varepsilon_2 = 0.40 \times 10^{-6}$$

$$\beta = 109.5^\circ$$

The result describes the original hypothetical shear-strain increment reasonably well. A trial with a rounding to 1×10^{-8} results in almost complete duplication of the hypothetical strain increment.

The likelihood ratio test of the preceding section can be used to estimate the required number of measurements to achieve a given level of accuracy at a given confidence level. We use the standard deviation of individual range ratio measurements of 5×10^{-7} as estimated from the present data (Table 3, excluding San Juan). Thus, substituting $\sigma_1 = \sigma_2 = 10^{-6}$ and $|\mu_1 - \mu_2| = 10^{-7}$ into eq. (18), we find that $n_1 = n_2 = 200$ will give $t \doteq 1.99$, which exceeds the value of t distribution, 1.97, for 198 degrees of freedom at 95% confidence level. Thus a variation in the range ratio of 10^{-7} found by averaging 200 ratio measurements is significant at 95% level of confidence.

At a rate of one measurement every hour, it will take slightly more than a week to complete this many measurements. Two such series of measurements one year apart is sufficient to determine the shear strain increment in southern California.

For a given set of t and σ's, n's are approximately inversely proportional to the square of the difference in μ's in equation (18). Thus doubling the measurement interval, thereby doubling the expected ratio variations, approximately quarters the required number of measurements. For example, a pair of 50-measurement sets two years apart will give the shear strain rate in southern California.

V. CONCLUSIONS AND RECOMMENDATIONS

Conclusions

Even though the field experiment we performed during this contract was quite limited compared with our original plan, we obtained several interesting and important results. The following is a list of conclusions drawn from these results:

1. The increment of the ratio of the length of a survey line to the average of several survey lines in a region is directly related to the incremental shear strain in the region. Thus, the shear strain rate can be calculated from observations of temporal variations in such ratios.

2. Using the TLRS, the time-of-flight ratios could be determined to an accuracy (one standard deviation) of 1×10^{-7} by averaging measurements over a four day period. This accuracy was obtained without using any atmospheric corrections at all. No improvement was obtained when atmospheric corrections based on end-point measurements were applied.

3. A calculation using a hypothetical data simulating the observed strain field in southern California indicates that two sets of TLRS ratio measurements separated by one to two years will be sufficient to determine the direction and rate of shear strain in the region.

4. Thus relative lateration using the TLRS has been demonstrated to be a good method for monitoring the regional shear strain field around satellite ranging stations. The TLRS operates successfully over long distances. The ratio method is extremely economical. It requires no environmental measurements and can be performed with small unattended retroreflectors distributed over a wide area. Thus these techniques greatly surpass the capability of conventional EDM techniques.

Recommendations

1. The results of the present experiment are thus very encouraging. However, they are based on only one experiment. Before this technique is put to a practical use, further demonstration is needed to confirm the above results. Therefore, it is recommended that this feasibility study be continued at least to include reoccupation of the Mt. Wilson site and two measurements at another properly selected site, preferably with a different meteorological environment.

2. Relative lateration is not limited to the data taken by the TLRS. The data reduction procedure used in the present study can be applied to other data from distance measurements. Therefore, it is recommended that we reanalyze some of existing ranging data to see if improvements in determination of shear strain rate can be achieved. This can be done without further field measurements.

3. Additional feasibility test measurements similar to the Mt. Wilson experiment may be obtained from fixed satellite ranging stations. It is therefore, recommended that this possibility be examined.

4. Horizontal ranging to distant targets on the ground does not require all the sophistication of the TLRS system. Therefore, when the capability of the present technique is fully demonstrated, a smaller, more portable single-photon ranging unit should be developed for this purpose.

5. Finally, the technology is advancing in other fields also. Such techniques as miniature interferometer terminals [Counselman and Shapiro, 1979] may someday be more useful in surveys of regional extent. Therefore, development in these other techniques should be reviewed while developing the present technique.

Acknowledgements

The initial data reduction of the Mt. Wilson experiment was done in the Astronomy Department of the University of Texas at Austin. We are grateful to Dr. Eric C. Silverberg for supplying us the processed data on a computer tape. Dr. Cliff Frohlich kindly reviewed a draft of this report, his constructive comments are greatly appreciated.

References

American Institute of Physics Handbook, 3rd ed., McGraw-Hill, New York, 1972.

Carter, W. E. and T. Vincenty, Survey of the McDonald Observatory radial line scheme by relative lateration technique, NOAA Technical Report NOS 74 NGS 9, 1978.

Counselman III, C.C. and I.I. Shapiro, Miniature interferometer terminals for earth surveying, Bull. Geod. 53, 139-163, 1973.

Huggett, G. R. and L. E. Slater, Precision electromagnetic distance-measuring instrument for determining secular strain and fault movement, Tectonophysics, 29, 19-27, 1975.

Huggett, G. R., L. E. Slater and J. Langbein, Fault slip episodes near Hollister, California: Initial results using a multiwavelength distance-measuring instrument, J. Geophys. Res., 82, 3361-3368, 1977.

Robertson, K. D., The use of line pairs in trilateration and traverse, Survey Rev., 21, 290-306, 1972.

Savage, J. C. and W. H. Prescott, Precision of Geodolite distance measurements for determining fault movements, J. Geophys. Res., 78, 6001-6008, 1973.

Savage, J. C., W. H. Prescott, M. Lisowski and N. E. King, Strain accumulation in southern California, 1973-1980, J. Geophys. Res., 86, 6991-7001, 1981.

Silverberg, E. C., and D. L. Byrd, A mobile telescope for measuring continental drift, Sky and Telescope, 61, 405-408, 1981.

Silverberg, E. C., T. Cahill and J. Dorman, Relative lateration across the Los Angeles basin using a satellite laser raning system, Bull. Geod., (in press), 1982.

Slater, L. E. and G. R. Huggett, A multiwavelength distance-measuring instrument for geophysical experiments, J. Geophys. Res., 81, 6299-6306, 1976.

APPENDIX

ORIGINAL PAGE IS
OF POOR QUALITY

Table A1. Calibrated Round-Trip Time of Flight

Castro					San Pedro					Niguel					Santiago					San Juan				
dy	hr	mn	sc	ns	dy	hr	mn	sc	ns	dy	hr	mn	sc	ns	dy	hr	mn	sc	ns	dy	hr	mn	sc	ns
22	10	04	29	456364.7	22	10	18	55	391913.7	24	04	28	32	563581.8	22	10	41	41	500003.1	22	10	51	17	303845.7
22	12	02	41	456365.9	22	12	21	52	391914.8	24	06	19	58	563582.6	22	12	43	11	500003.8	22	12	51	51	303846.2
22	14	05	43	456365.6	22	14	15	03	391914.4	24	06	46	28	563581.9	22	14	34	32	500003.5	22	14	48	04	303846.4
23	00	09	40	456366.5	22	18	23	39	391915.5	24	08	18	26	563582.0	22	22	49	55	500004.4	22	18	55	03	303847.6
23	02	09	25	456366.3	24	04	20	40	391917.4	24	10	15	13	563581.9	23	00	41	06	500004.8	22	22	54	59	303847.4
23	06	05	03	456366.5	24	06	16	19	391918.0	24	10	40	16	563582.1	23	04	33	04	500004.5	23	06	47	01	303847.3
24	06	08	46	456369.4	24	06	51	04	391917.8	24	14	15	10	563582.0	23	06	39	34	500004.4	23	08	47	14	303847.0
24	06	58	17	456369.4	24	08	09	40	391918.0	24	14	40	18	563582.2	23	08	39	44	500004.0	24	04	40	14	303849.0
24	08	00	19	456369.2	24	10	10	03	391917.6	24	16	18	20	563581.8	24	04	40	08	500007.4	24	06	29	45	303849.1
24	09	59	54	456369.1	24	10	45	34	391917.7	25	02	21	58	563581.2	24	06	25	43	500007.6	24	06	33	37	303849.6
24	10	55	03	456369.3	24	12	10	04	391917.8	25	02	48	49	563581.2	24	06	41	31	500007.4	24	08	25	49	303849.4
24	12	00	58	456369.4	24	14	11	30	391917.8	25	10	16	05	563579.8	24	08	22	17	500007.6	24	12	25	08	303849.2
24	14	01	34	456369.2	24	14	45	60	391917.6	25	10	41	13	563579.6	24	10	21	13	500007.3	24	14	25	20	303849.8
24	14	55	05	456369.8	25	02	13	18	391917.0						24	10	35	15	500007.5	24	14	35	04	303849.9
24	16	01	03	456369.7	25	02	53	27	391917.6						24	12	20	03	500007.4	24	16	28	54	303849.6
24	18	00	06	456369.2	25	04	09	53	391917.0						24	14	20	03	500006.8	25	02	33	03	303849.0
24	18	57	39	456369.0	25	06	10	05	391916.6						24	14	35	11	500006.8	25	02	36	56	303849.0
24	22	44	42	456368.4	25	06	45	43	391916.4						24	16	29	53	500007.0	25	04	25	60	303849.6
25	02	05	25	456368.8	25	08	11	36	391916.5						24	20	18	04	500006.6	25	06	32	42	303849.4
25	02	58	04	456369.2	25	10	10	16	391916.4						25	00	25	13	500006.0	25	08	23	56	303847.8
25	04	00	52	456368.6	25	10	45	23	391916.0						25	02	29	30	500006.6	25	10	23	11	303847.6
25	06	01	17	456368.6	25	12	10	30	391916.6						25	02	39	51	500006.6	25	10	35	03	303847.8
25	06	55	21	456368.4	25	14	15	11	391916.8						25	04	22	37	500007.0	25	12	25	03	303849.0
25	08	04	49	456367.7	25	14	40	42	391916.8						25	06	22	51	500006.4	25	18	31	55	303847.8
25	10	01	53	456367.6											25	06	35	48	500006.0	25	20	25	59	303848.4
25	10	55	08	456367.8											25	08	20	32	500005.6	25	22	23	50	303847.2
25	12	04	05	456367.5											25	10	20	08	500005.4	26	00	32	50	303847.6
25	14	51	54	456368.4											25	10	35	11	500065.2					
25	16	00	28	456368.2											25	12	21	02	500005.2					
25	18	00	19	456367.9											25	14	21	41	500005.8					
25	18	59	43	456368.0											25	14	35	02	500005.8					
25	20	07	42	456367.9											25	16	20	06	500006.2					
25	20	37	24	456367.7											25	18	39	42	500006.0					
25	20	49	58	456368.1											25	20	20	59	500005.9					
25	22	51	57	456367.1											25	22	37	54	500005.4					
26	00	05	27	456367.2											26	00	26	53	500005.4					

ORIGINAL PAGE IS OF POOR QUALITY

Table A2. Temperature, T, Pressure, P, and Saturated Vapor Pressure, V

Time dy	hr	mn	sc	T deg C	P mmHg	V mmHg
Mt. Wilson						
22	12	08	01	8.0	624.1	8.0422
22	13	08	54	7.0	624.1	7.5104
22	14	53	40	8.0	624.8	8.0422
22	15	59	57	8.0	624.8	8.0422
22	16	31	16	9.0	624.8	8.6062
22	16	57	27	8.0	624.8	8.0422
22	17	59	44	10.0	625.6	9.2048
22	19	14	19	12.0	624.8	10.5136
22	21	57	23	10.0	623.3	9.2048
22	22	25	11	11.0	624.1	9.8401
22	23	02	15	10.0	623.3	9.2048
23	00	00	56	9.0	623.3	8.6062
23	00	28	23	8.0	623.3	8.0422
23	01	03	14	8.0	623.3	8.0422
23	02	01	37	7.0	623.3	7.5104
23	02	24	05	7.0	623.3	7.5104
23	02	48	26	6.0	623.3	7.0108
23	04	13	00	6.0	623.3	7.0108
23	04	53	34	5.0	623.3	6.5398
23	05	57	22	5.0	624.1	6.5398
23	06	37	07	5.0	623.3	6.5398
23	06	55	29	6.0	623.3	7.0108
23	07	52	58	5.0	622.6	6.5398
23	08	20	32	5.0	622.6	6.5398
23	08	54	34	5.0	622.6	6.5398
23	09	56	13	4.0	622.6	6.0973
23	10	29	17	4.0	622.6	6.0973
23	10	55	37	3.0	621.8	5.6817
24	04	06	03	0.0	622.6	4.5814
24	04	22	39	-1.0	622.6	4.2589
24	04	55	29	0.0	622.6	4.5814
24	05	56	14	0.0	622.6	4.5814
24	06	34	27	-1.0	622.6	4.2589
24	07	04	10	0.0	622.6	4.5814
24	07	51	41	-1.0	622.6	4.2589
24	08	31	26	-1.0	622.6	4.2589
24	09	46	20	0.0	622.6	4.5814
24	10	28	48	-1.0	621.8	4.2589
24	11	00	43	-1.0	622.6	4.2589
24	11	55	50	-1.0	622.6	4.2589
24	12	34	12	-1.0	621.8	4.2589

Time dy	hr	mn	sc	T deg C	P mmHg	V mmHg
24	13	54	08	0.0	621.8	4.5814
24	14	28	00	0.0	621.8	4.5814
24	14	54	16	0.0	621.8	4.5814
24	15	53	54	0.0	622.6	4.5814
24	16	41	49	2.0	622.6	5.2917
24	17	53	26	3.0	623.3	5.6817
24	19	06	29	4.0	622.6	6.0973
24	19	55	54	4.0	622.6	6.0973
24	20	49	38	5.0	621.8	6.5398
24	21	54	25	6.0	620.3	7.0108
24	22	27	53	6.0	620.3	7.0108
24	22	52	51	6.0	620.3	7.0108
24	23	55	10	4.0	620.3	6.0973
25	00	34	16	5.0	620.3	6.5398
25	02	00	11	2.0	620.3	5.2917
25	03	03	19	1.0	620.3	4.9249
25	03	55	51	0.0	620.3	4.5814
25	04	32	31	1.0	620.3	4.9249
25	05	54	44	1.0	620.3	4.9249
25	06	28	44	1.0	620.3	4.9249
25	07	01	06	1.0	620.3	4.9249
25	07	56	42	0.0	619.6	4.5814
25	08	36	19	0.0	618.8	4.5814
25	09	48	16	1.0	618.8	4.9249
25	10	28	22	2.0	618.8	5.2917
25	11	00	51	2.0	618.1	5.2917
25	11	59	30	0.0	618.1	4.5814
25	12	34	14	1.0	618.1	4.9249
25	13	57	00	2.0	618.1	5.2917
25	14	26	09	1.0	618.1	4.9249
25	14	56	49	1.6	618.8	4.9249
25	15	55	10	2.0	619.6	5.2917
25	16	36	22	3.0	619.6	5.6817
25	17	55	39	5.0	619.6	6.5398
25	18	45	58	6.0	619.6	7.0108
25	19	05	52	6.0	618.8	7.0108
25	19	55	15	7.0	618.8	7.5104
25	20	31	54	7.0	618.8	7.5104
25	21	06	50	8.0	618.8	8.0422
25	21	54	44	7.0	618.1	7.5104
25	22	32	53	8.0	618.1	8.0422
25	23	02	07	7.0	618.1	7.5104
25	23	48	19	4.0	618.8	6.0973
26	00	36	21	6.0	618.8	7.0108

Time dy	hr	mn	sc	T deg C	P mmHg	V mmHg
26	01	08	09	4.0	616.8	6.0973
27	21	13	23	0.0	619.6	4.5814
Castro						
22	09	10	00	14.4	690.8	8.0724
22	10	00	00	14.2	690.1	9.2050
22	11	00	00	13.5	690.1	8.3828
22	12	00	00	13.6	690.8	9.2050
22	13	00	00	13.4	690.1	7.9210
22	14	00	00	13.3	690.8	7.6258
22	15	00	00	13.2	690.8	7.7721
22	16	00	00	13.8	690.8	7.9210
22	17	00	00	14.0	691.6	7.9210
22	18	00	00	14.9	691.6	8.2263
22	19	00	00	15.8	691.6	7.9210
22	20	00	00	18.8	690.8	9.5532
22	21	00	00	15.9	690.1	9.5532
22	22	00	00	14.8	690.1	10.2856
22	23	00	00	15.8	690.1	11.4747
23	00	00	00	13.9	690.1	8.5418
23	01	00	00	12.7	690.1	7.9210
23	02	00	00	11.8	690.8	7.6258
23	03	00	00	10.4	690.8	7.9210
23	04	00	00	11.7	690.1	7.3403
23	05	00	00	11.5	690.1	7.6258
23	06	00	00	11.4	690.1	7.6258
23	16	00	00	6.6	692.3	7.6645
23	17	00	00	8.5	693.1	8.0724
23	18	00	00	10.3	693.1	8.8679
23	19	00	00	12.2	693.1	9.9131
23	20	00	00	10.1	693.1	8.8679
23	21	00	00	9.3	692.3	8.5418
23	22	00	00	11.1	692.3	8.8679
23	23	00	00	10.6	692.3	8.8679
24	00	00	00	8.9	692.3	8.2263
24	01	00	00	7.3	692.3	7.3403
24	02	00	00	5.9	692.3	6.7978
24	03	00	00	5.8	692.3	7.0645
24	04	00	00	5.8	693.1	6.7978
24	05	00	00	5.9	693.1	6.7978
24	06	00	00	6.0	693.1	6.5400
24	07	00	00	6.3	693.8	6.5400
24	08	00	00	6.5	693.8	6.5400

Table A2. (continued)

dy	hr	mn	sc	T deg C	P mmHg	V mmHg
24	09	00	00	6.1	693.1	6.2908
24	10	00	00	5.9	693.1	6.0500
24	11	00	00	5.8	693.1	5.8176
24	12	00	00	6.0	693.1	5.8176
24	13	00	00	5.8	693.1	5.8176
24	14	00	00	5.5	693.1	5.5931
24	15	00	00	5.1	693.1	5.5931
24	16	00	00	5.6	693.1	5.8176
24	17	00	00	6.8	693.1	6.5400
24	18	00	00	8.2	693.1	6.7978
24	19	00	00	9.3	693.1	7.2012
24	20	00	00	11.2	692.3	7.6258
24	21	00	00	12.0	691.6	7.6258
24	22	00	00	11.0	691.6	8.2263
24	23	00	00	12.0	690.8	8.2263
25	00	00	00	10.3	690.8	7.3403
25	01	00	00	6.6	690.8	6.0500
25	02	00	00	5.8	690.1	6.0500
25	03	00	00	5.7	690.1	6.5400
25	04	00	00	5.3	690.8	5.8176
25	05	00	00	5.7	690.8	5.3762
25	06	00	00	5.7	690.1	5.1669
25	07	00	00	5.0	690.1	5.3762
25	08	00	00	5.6	689.3	5.3762
25	09	00	00	5.5	689.3	5.3762
25	10	00	00	5.3	689.3	5.3762
25	11	00	00	5.3	689.3	5.5931
25	12	00	00	4.7	689.3	5.3762
25	13	00	00	5.5	688.6	5.8176
25	14	00	00	5.2	689.3	5.3762
25	15	00	00	5.3	690.1	5.5931
25	16	00	00	5.4	690.8	5.3762
25	17	00	00	7.3	690.8	5.9327
25	18	00	00	8.5	690.8	6.2908
25	19	00	00	10.0	690.8	6.6678
25	20	00	00	12.3	690.1	6.7978
25	21	00	00	16.2	689.3	8.2263
25	22	00	00	14.1	688.6	6.5400
25	23	00	00	16.1	689.3	7.3403
26	00	00	00	12.5	690.1	6.7978

San Pedro

dy	hr	mn	sc	T deg C	P mmHg	V mmHg
22	10	21	00	14.7	718.6	9.9131

dy	hr	mn	sc	T deg C	P mmHg	V mmHg
22	12	20	00	13.4	719.3	9.2050
22	14	20	00	12.6	720.1	9.2050
22	16	20	00	15.6	720.1	9.9131
22	18	20	00	19.1	720.8	10.6688
22	22	00	00	18.7	719.3	11.8118
23	10	30	00	11.5	718.6	
23	16	20	00	12.1	720.8	9.5532
23	18	20	00	12.4	720.8	10.2850
23	20	30	00	14.7	720.8	11.8974
24	00	30	00	11.3	720.1	9.3777
24	04	20	00	9.1	720.8	8.6708
24	06	10	00	9.4	720.8	8.8679
24	06	45	00	9.3	720.8	8.7361
24	08	10	00	9.0	720.1	7.7721
24	10	10	00	8.3	720.1	8.2263
24	10	45	00	8.2	720.1	7.8610
24	12	10	00	8.6	720.1	7.7721
24	14	10	00	8.4	720.1	7.6258
24	14	45	00	8.1	720.1	7.6258
25	02	10	00	9.8	719.3	8.5418
25	02	52	00	9.8	719.3	8.7036
25	04	10	00	9.8	719.3	8.2263
25	06	10	00	9.4	720.1	6.7978
25	06	46	00	8.6	718.6	6.4143
25	08	10	00	7.8	718.6	6.0500
25	10	10	00	8.8	718.6	6.7978
25	10	45	00	8.8	718.6	6.7978
25	12	10	00	7.8	718.6	6.2908
25	14	10	00	7.8	717.8	7.0645
25	14	22	00	7.6	718.6	6.7978
25	16	10	00	11.4	719.3	

Niguel

dy	hr	mn	sc	T deg C	P mmHg	V mmHg
22	09	28	00	13.2	738.8	8.8679
22	10	32	00	12.5	738.8	9.2050
22	11	30	00	12.0	738.8	9.2050
22	12	30	00	11.4	738.8	9.2050
22	13	31	00	11.5	738.8	9.7318
22	14	30	00	14.1	739.6	9.9131
22	15	41	00	13.6	740.3	9.5532
22	16	36	00	15.0	740.3	10.6688
22	17	30	00	16.2	740.3	11.0653
22	18	31	00	17.1	740.3	12.3337

dy	hr	mn	sc	T deg C	P mmHg	V mmHg
22	19	33	00	18.1	740.3	11.8974
22	20	32	00	19.2	739.6	12.3337
22	21	40	00	16.7	738.8	13.2406
22	22	30	00	15.3	738.8	11.8974
22	23	37	00	13.9	739.6	11.4747
23	00	38	00	13.1	739.6	11.0653
23	01	45	00	11.6	739.6	11.0653
23	02	32	00	12.3	739.6	10.6688
23	03	35	00	11.6	739.6	10.2850
23	04	40	00	11.7	739.5	10.2850
23	05	30	00	11.6	739.6	10.2850
23	06	32	00	11.2	738.8	9.9131
23	07	30	00	11.3	738.6	9.9131
23	08	30	00	14.1	738.1	9.5532
23	09	29	00	12.7	738.8	10.6688
23	10	35	00	12.4	738.8	10.2850
23	11	30	00	12.4	738.8	10.2850
23	12	40	00	12.5	738.8	10.2850
23	17	40	00	13.1	741.8	11.4747
23	18	34	00	13.5	741.8	13.2486
23	19	30	00	13.5	741.8	11.0653
23	20	40	00	16.3	741.1	12.3337
23	21	33	00	16.0	741.1	11.4747
23	22	30	00	15.5	741.1	11.4747
23	23	26	00	16.2	741.1	11.0653
24	00	30	00	13.0	741.1	9.9131
24	01	40	00	11.0	741.8	9.2050
24	02	40	00	10.7	741.8	9.2050
24	03	50	00	10.8	741.8	9.2050
24	04	35	00	10.7	741.8	9.2050
24	05	40	00	10.3	741.8	9.2050
24	06	20	00	10.3	741.8	8.8679
24	07	35	00	10.2	741.8	8.8679
24	08	35	00	9.7	741.8	8.5418
24	09	30	00	10.4	741.1	9.2050
24	10	30	00	9.2	741.1	8.5418
24	11	39	00	8.5	741.1	8.2263
24	12	31	00	8.4	741.1	8.2263
24	13	33	00	8.0	740.3	7.9210
24	14	31	00	7.7	740.3	7.6258
24	15	35	00	9.3	740.3	8.5418
24	16	17	00	10.6	741.1	9.2050
24	17	20	00	13.6	741.1	9.9131
24	18	17	00	13.5	741.1	9.9131

Table A2. (continued)

Time dy hr mn sc	T deg C	P mmHg	V mmHg	Time dy hr mn sc	T deg C	P mmHg	V mmHg	Time dy hr mn sc	T deg C	P mmHg	V mmHg
24 19 15 00	14.2	740.3	10.2850	22 14 40 00	9.8	623.3	5.3762	24 05 45 00	1.0	622.6	
24 20 23 00	16.0	738.8	11.0653	22 15 00 00	10.2	623.3		24 06 25 00	1.1	622.6	4.3764
24 21 40 00	16.1	738.1	10.6688	22 16 30 00	10.0	624.1	5.7043	24 06 40 00	1.2	622.6	4.2774
24 22 30 00	15.5	738.1	10.2850	22 16 45 00	10.0	624.1	5.5931	24 07 40 00	.7	621.8	
24 23 30 00	15.4	738.1	10.2850	22 17 30 00	10.0	624.1		24 08 20 00	.8	621.8	4.5811
25 00 27 00	13.1	738.1	9.0350	22 18 00 00	10.8	624.1	6.5400	24 09 20 00	.5	621.8	4.4780
25 01 15 00	11.0	738.1	8.8679	22 18 45 00	13.0	624.1	7.3403	24 10 20 00	.8	621.1	4.1783
25 02 27 00	9.4	738.1	8.2263	22 19 00 00	13.0	624.1		24 11 20 00	.4	621.1	
25 03 30 00	8.4	738.1	7.6258	22 20 00 00	12.5	623.3		24 12 20 00	.8	621.1	3.8100
25 04 23 00	7.9	738.1	7.3403	22 21 00 00	13.0	622.6		24 13 20 00	.8	621.1	
25 05 40 00	8.8	737.3	6.7978	22 22 00 00	11.6	622.6	6.2908	24 14 20 00	1.8	621.1	4.5811
25 06 25 00	8.9	737.3	6.7978	22 22 45 00	10.3	622.6		24 15 20 00	3.2	621.1	
25 07 28 00	8.5	737.3	6.5400	22 23 00 00	11.0	622.6		24 16 20 00	2.2	621.1	4.0943
25 08 23 00	8.7	736.6	6.7978	22 23 45 00	9.2	623.3	7.0645	24 17 20 00	3.5	621.8	
25 09 29 00	8.3	735.8	6.7978	23 00 00 00	9.2	621.8		24 18 20 00	3.4	621.8	5.0648
25 10 30 00	8.4	735.8	6.7978	23 00 45 00	7.2	621.8	6.0500	24 18 37 00	3.8	621.8	
25 11 35 00	8.5	735.8	7.0645	23 01 00 00	8.0	621.8		24 19 20 00	5.2	621.1	7.6258
25 12 29 00	8.0	735.8	7.3403	23 02 00 00	7.2	622.6		24 20 00 00	5.4	621.1	5.8176
25 13 30 00	7.9	735.8	7.0645	23 02 45 00	7.7	622.6	6.5400	24 20 15 00	6.3	621.1	
25 14 25 00	7.1	735.8	7.6258	23 03 00 00	7.3	622.6		24 20 30 00	7.1	620.3	
25 15 30 00	8.9	736.6	7.6258	23 04 00 00	6.2	622.6		24 20 40 00	7.3	620.3	6.4397
25 16 17 00	11.1	737.3	8.8679	23 04 45 00	6.2	622.6		24 20 50 00	7.5	620.3	
25 17 15 00	12.3	738.1	9.2050	23 05 00 00	6.5	622.6		24 21 00 00	8.8	620.3	
25 18 16 00	14.1	737.3	10.2850	23 06 00 00	6.5	622.6	5.4836	24 21 05 00	7.5	619.6	
25 19 24 00	15.1	735.8	10.2850	23 06 40 00	6.8	622.6	6.2908	24 21 15 00	7.9	619.6	
25 20 20 00	16.0	735.1	10.6688	23 07 00 00	7.0	622.6		24 22 00 00	8.7	619.6	
25 21 24 00	16.0	735.1	9.9131	23 08 00 00	7.3	621.8		24 22 15 00	8.9	619.6	7.0645
25 22 20 00	16.9	734.3	10.6688	23 08 40 00	7.7	621.1	4.9647	24 22 20 00	8.8	619.6	
25 23 26 00	15.3	734.3	10.2850	23 08 45 00	7.9	621.1		24 22 23 00	9.4	619.6	
26 00 20 00	14.4	735.1	9.9131	23 09 00 00	8.0	621.1		24 22 32 00	7.9	619.6	7.2012
				23 10 00 00	4.8	621.1		24 22 35 00	7.5	619.6	
Santiago				23 11 00 00	5.1	621.1		24 22 45 00	6.9	619.6	6.6937
				23 12 00 00	4.4	621.1		24 23 15 00	5.4	619.6	
22 09 00 00	11.0	623.3		23 12 45 00	4.6	621.1		24 23 35 00	5.0	619.6	
22 10 00 00	10.3	623.3	5.5710	23 19 30 00	4.9	622.6	5.3762	25 00 15 00	4.3	618.8	5.0648
22 10 40 00	10.1	623.3		23 20 00 00	5.1	622.6		25 00 20 00	4.0	619.6	
22 10 46 00	10.2	623.3		23 21 00 00	5.5	621.8		25 00 25 00	3.8	619.6	
22 11 00 00	12.4	623.3		23 22 00 00	4.2	621.8		25 00 29 00	3.9	618.8	
22 12 00 00	10.2	622.6		23 23 00 00	2.2	621.8		25 01 15 00	2.8	618.8	
22 12 42 00	10.5	623.3		24 00 00 00	1.4	621.8		25 01 20 00	2.7	618.8	
22 12 46 00	10.3	623.3		24 01 45 00	1.0	621.8		25 02 15 00	2.4	618.8	4.7696
22 12 50 00	10.3	623.3		24 02 45 00	1.0	621.8		25 02 27 00	2.3	618.8	
22 13 00 00	10.0	623.3		24 03 45 00	1.0	622.6		25 02 32 00	2.5	618.8	
22 14 00 00	9.8	623.3		24 04 45 00	.8	622.6	4.3764	25 02 39 00	2.3	618.0	

Table A2. (continued)

Time dy hr mn sc	T deg C	P mmHg	V mmHg
25 02 43 00	2.3	618.8	
25 02 51 00	2.4	618.8	4.7315
25 03 00 00	2.3	618.8	
25 03 15 00	1.7	618.8	
25 03 27 00	1.5	618.8	
25 04 15 00	1.1	618.8	4.5811
25 04 25 00	1.0	618.8	
25 05 15 00	.5	618.8	
25 05 25 00	.8	618.8	
25 06 15 00	1.8	618.8	
25 06 23 00	2.1	618.8	4.5811
25 06 26 00	2.0	618.8	
25 06 35 00	1.9	618.8	
25 06 37 00	1.9	618.8	
25 06 50 00	2.1	618.8	
25 07 15 00	2.3	618.8	
25 07 25 00	2.8	618.1	
25 08 15 00	.6	618.1	4.3764
25 08 20 00	.2	618.1	
25 08 24 00	.1	618.1	
25 09 20 00	1.1	617.3	
25 10 15 00	1.9	617.3	
25 10 20 00	1.8	617.3	
25 10 23 00	1.8	617.3	4.2774
25 10 35 00	1.6	617.3	
25 10 38 00	1.7	617.3	
25 10 50 00	1.8	617.3	
25 11 15 00	2.1	617.3	
25 11 20 00	2.1	617.3	
25 12 15 00	.8	616.6	3.8100
25 12 20 00	.3	616.6	4.3764
25 12 23 00	.4	616.6	
25 13 15 00	.6	617.3	
25 13 20 00	.5	617.3	
25 14 20 00	-.3	617.3	4.3764
25 15 20 00	1.9	618.1	
25 16 20 00	4.7	618.1	
25 17 20 00	5.5	618.8	
25 18 20 00	6.2	618.8	6.0500
25 19 20 00	7.7	618.1	
25 20 20 00	8.3	617.3	6.2908
25 21 20 00	9.4	617.3	
25 22 20 00	8.8	617.3	
25 23 20 00	6.8	617.3	
26 00 20 00	5.5	617.3	6.1694

San Juan

Time dy hr mn sc	T deg C	P mmHg	V mmHg
22 08 00 00	16.0	717.8	9.0688
22 09 03 00	15.8	717.8	8.5418
22 10 02 00	15.3	717.8	9.1366
22 10 58 00	14.8	717.8	11.0251
22 11 58 00	16.0	717.8	9.6957
22 12 59 00	16.5	717.8	10.6299
22 14 26 00	15.8	717.8	11.0653
22 15 03 00	16.0	718.6	7.8610
22 16 05 00	15.5	719.3	7.8016
22 17 02 00	15.8	719.3	8.1643
22 18 00 00	19.3	719.3	8.5418
22 19 00 00	25.6	719.3	10.2850
22 20 02 00	22.2	718.6	10.2850
22 21 00 00	20.0	717.1	10.6688
22 22 00 00	18.5	717.1	11.4747
22 23 00 00	18.0	717.8	11.3916
23 00 00 00	15.0	717.8	10.0975
23 01 00 00	13.5	717.1	10.4752
23 02 00 00	12.0	717.8	9.9131
23 03 00 00	11.0	718.6	9.9131
23 04 10 00	12.0	718.6	9.5532
23 05 00 00	11.5	718.6	9.7318
23 06 00 00	11.0	717.8	9.5532
23 07 00 00	11.5	717.8	9.5532
23 08 02 00	12.0	717.1	9.3081
23 09 00 00	12.0	716.3	9.0350
23 10 00 00	10.5	717.1	9.2392
23 10 56 00	11.0	717.8	9.5179
23 12 03 00	11.5	717.8	9.4475
23 18 00 00	12.5	719.3	9.1026
23 19 00 00	15.5	719.3	9.5532
23 20 05 00	15.5	718.6	10.2850
23 21 00 00	13.0	718.6	9.9131
23 22 10 00	14.5	717.8	9.7318
23 23 05 00	12.0	717.8	9.2050
24 00 00 00	11.5	718.6	9.2050
24 01 00 00	11.5	718.6	9.0350
24 02 00 00	9.5	719.3	8.6385
24 03 00 00	9.0	719.3	8.2263
24 04 00 00	9.0	719.3	8.0724
24 04 45 00	8.5	719.3	8.3828
24 06 00 00	8.5	719.3	8.2263
24 06 30 00	8.0	719.3	8.0724
24 06 37 00	8.0	719.3	7.8313
24 08 28 00	8.6	719.3	7.6840
24 10 05 00	9.0	718.6	7.6258
24 11 01 00	8.0	718.6	7.3403
24 12 00 00	8.0	718.6	7.3403
24 13 10 00	8.0	718.6	7.1737
24 14 00 00	7.5	717.8	7.0645
24 15 02 00	7.0	717.8	7.0645
24 16 03 00	8.0	718.6	7.4534
24 16 33 00	8.6	718.6	7.6548
24 17 31 00	11.5	718.6	8.4778
24 18 29 00	13.2	717.8	9.7318
24 19 34 00	15.0	717.1	9.8402
24 20 30 00	16.5	716.3	9.7318
24 21 30 00	15.5	716.3	9.6350
24 22 30 00	16.9	715.6	9.5532
24 23 30 00	14.5	715.6	9.0350
25 00 30 00	12.0	715.6	8.0724
25 01 30 00	9.5	715.6	8.0724
25 02 36 00	8.5	715.6	7.9210
25 03 30 00	8.0	715.6	7.6258
25 04 35 00	8.5	715.6	7.8610
25 05 30 00	9.5	715.6	8.2885
25 06 35 00	8.2	715.6	7.0645
25 07 30 00	7.5	714.8	7.2012
25 08 32 00	8.0	714.1	6.0678
25 09 30 00	9.0	713.3	6.3894
25 10 31 00	10.0	713.3	6.1935
25 11 30 00	7.5	713.3	6.6678
25 12 31 00	7.5	713.3	6.7978
25 13 35 00	7.0	714.1	6.4394
25 14 29 00	7.0	714.1	6.0028
25 15 32 00	9.3	714.8	7.5969
25 16 32 00	11.0	715.6	8.5058
25 17 33 00	17.0	715.6	9.2050
25 18 33 00	14.4	714.8	8.5418
25 19 30 00	15.5	714.1	8.2263
25 20 35 00	18.0	713.3	8.3828
25 21 45 00	18.5	712.6	7.9210
25 22 33 00	20.0	712.6	7.6840
26 00 35 00	16.5	713.3	7.4818

ORIGINAL PAGE IS OF POOR QUALITY

Table A3. Group Index of Refraction at End Points

Time dy hr mn sc	n	Time dy hr mn sc	n	Time dy hr mn sc	n	Time dy hr mn sc	n
		24 13 54 08	1.00025008	26 01 08 09	1.00024528	24 09 00 00	1.00027267
Mt. Wilson		24 14 28 00	1.00025008	27 21 13 23	1.00024919	24 10 00 00	1.00027286
		24 14 54 16	1.00025008			24 11 00 00	1.00027296
22 12 08 01	1.00024386	24 15 53 54	1.00025040	Castro		24 12 00 00	1.00027276
22 13 08 54	1.00024473	24 16 41 49	1.00024858			24 13 00 00	1.00027296
22 14 53 40	1.00024414	24 17 53 26	1.00024796	22 09 10 00	1.00026392	24 14 00 00	1.00027325
22 15 59 57	1.00024414	24 19 06 29	1.00024679	22 10 00 00	1.00026383	24 15 00 00	1.00027365
22 16 31 16	1.00024327	24 19 55 54	1.00024679	22 11 00 00	1.00026448	24 16 00 00	1.00027315
22 16 57 27	1.00024414	24 20 49 38	1.00024558	22 12 00 00	1.00026465	24 17 00 00	1.00027198
22 17 59 44	1.00024272	24 21 54 25	1.00024411	22 13 00 00	1.00026457	24 18 00 00	1.00027063
22 19 14 19	1.00024071	24 22 27 53	1.00024411	22 14 00 00	1.00026493	24 19 00 00	1.00026958
22 21 57 23	1.00024183	24 22 52 51	1.00024411	22 15 00 00	1.00026502	24 20 00 00	1.00026747
22 22 25 11	1.00024129	24 23 55 10	1.00024588	22 16 00 00	1.00026447	24 21 00 00	1.00026645
22 23 02 15	1.00024183	25 00 34 16	1.00024499	22 17 00 00	1.00026459	24 22 00 00	1.00026738
23 00 00 56	1.00024269	25 02 00 11	1.00024766	22 18 00 00	1.00026376	24 23 00 00	1.00026614
23 00 28 23	1.00024355	25 03 03 19	1.00024857	22 19 00 00	1.00026294	25 00 00 00	1.00026773
23 01 03 14	1.00024355	25 03 55 51	1.00024948	22 20 00 00	1.00025994	25 01 00 00	1.00027128
23 02 01 37	1.00024442	25 04 32 31	1.00024857	22 21 00 00	1.00026228	25 02 00 00	1.00027178
23 02 24 05	1.00024442	25 05 54 44	1.00024857	22 22 00 00	1.00026328	25 03 00 00	1.00027187
23 02 48 26	1.00024529	25 06 28 44	1.00024857	22 23 00 00	1.00026237	25 04 00 00	1.00027254
23 04 13 00	1.00024529	25 07 01 06	1.00024857	23 00 00 00	1.00026411	25 05 00 00	1.00027215
23 04 53 34	1.00024618	25 07 56 42	1.00024919	23 01 00 00	1.00026522	25 06 00 00	1.00027187
23 05 57 22	1.00024649	25 08 36 19	1.00024887	23 02 00 00	1.00026632	25 07 00 00	1.00027256
23 06 37 07	1.00024618	25 09 48 16	1.00024796	23 03 00 00	1.00026764	25 08 00 00	1.00027166
23 06 55 29	1.00024529	25 10 28 22	1.00024706	23 04 00 00	1.00026615	25 09 00 00	1.00027175
23 07 52 58	1.00024590	25 11 00 51	1.00024678	23 05 00 00	1.00026634	25 10 00 00	1.00027195
23 08 20 32	1.00024590	25 11 59 30	1.00024859	23 06 00 00	1.00026643	25 11 00 00	1.00027195
23 08 54 34	1.00024590	25 12 34 14	1.00024768	23 16 00 00	1.00027186	25 12 00 00	1.00027254
23 09 56 13	1.00024679	25 13 57 00	1.00024678	23 17 00 00	1.00027034	25 13 00 00	1.00027148
23 10 29 17	1.00024679	25 14 26 09	1.00024768	23 18 00 00	1.00026863	25 14 00 00	1.00027205
23 10 55 37	1.00024736	25 14 56 49	1.00024796	23 19 00 00	1.00026684	25 15 00 00	1.00027227
24 04 06 03	1.00025040	25 15 55 10	1.00024738	23 20 00 00	1.00026882	25 16 00 00	1.00027244
24 04 22 39	1.00025132	25 16 36 22	1.00024649	23 21 00 00	1.00026927	25 17 00 00	1.00027660
24 04 55 29	1.00025040	25 17 55 39	1.00024471	23 22 00 00	1.00026756	25 18 00 00	1.00026945
24 05 56 14	1.00025040	25 18 45 58	1.00024384	23 23 00 00	1.00026803	25 19 00 00	1.00026802
24 06 34 27	1.00025132	25 19 05 52	1.00024352	24 00 00 00	1.00026965	25 20 00 00	1.00026559
24 07 04 10	1.00025040	25 19 55 15	1.00024265	24 01 00 00	1.00027119	25 21 00 00	1.00026171
24 07 51 41	1.00025132	25 20 31 54	1.00024265	24 02 00 00	1.00027255	25 22 00 00	1.00026335
24 08 31 26	1.00025132	25 21 06 50	1.00024179	24 03 00 00	1.00027264	25 23 00 00	1.00026180
24 09 46 20	1.00025040	25 21 54 44	1.00024238	24 04 00 00	1.00027296	26 00 00 00	1.00026540
24 10 28 48	1.00025100	25 22 32 53	1.00024152	24 05 00 00	1.00027286		
24 11 00 43	1.00025132	25 23 02 07	1.00024238	24 06 00 00	1.00027276	San Pedro	
24 11 55 50	1.00025132	25 23 48 19	1.00024528	24 07 00 00	1.00027275		
24 12 34 12	1.00025100	26 00 36 21	1.00024352	24 08 00 00	1.00027255	22 10 21 00	1.00027425

Table A3. (continued)

Time dy hr mn sc	n	Time dy hr mn sc	n	Time dy hr mn sc	n	Time dy hr mn sc	n
22 12 20 00	1.00027576	22 19 33 00	1.00027924	24 19 15 00	1.00028302	22 14 49 00	1.00024200
22 14 20 00	1.00027684	22 20 32 00	1.00027792	24 20 23 00	1.00028069	22 15 00 00	1.00024166
22 16 20 00	1.00027397	22 21 40 00	1.00028002	24 21 40 00	1.00028033	22 16 00 00	1.00024214
22 18 20 00	1.00027095	22 22 30 00	1.00028137	24 22 30 00	1.00028091	22 16 45 00	1.00024214
22 22 00 00	1.00027076	22 23 37 00	1.00028305	24 23 30 00	1.00028101	22 17 00 00	1.00024214
23 10 20 00	1.00027733	23 00 38 00	1.00028384	25 00 27 00	1.00028327	22 18 00 00	1.00024146
23 16 20 00	1.00027760	23 01 45 00	1.00028534	25 01 15 00	1.00028536	22 18 45 00	1.00023960
23 18 20 00	1.00027731	23 02 32 00	1.00028464	25 02 27 00	1.00028698	22 19 00 00	1.00023960
23 20 30 00	1.00027509	23 03 35 00	1.00028534	25 03 30 00	1.00028800	22 20 00 00	1.00023971
24 00 20 00	1.00027811	23 04 40 00	1.00028524	25 04 23 00	1.00028851	22 21 00 00	1.00023903
24 04 20 00	1.00028055	23 05 30 00	1.00028534	25 05 40 00	1.00028728	22 22 00 00	1.00024020
24 06 10 00	1.00028025	23 06 32 00	1.00028543	25 06 25 00	1.00028717	22 22 45 00	1.00024130
24 06 45 00	1.00028035	23 07 30 00	1.00028533	25 07 28 00	1.00028758	22 23 00 00	1.00024071
24 08 10 00	1.00028038	23 08 30 00	1.00028228	25 08 23 00	1.00028711	22 23 45 00	1.00024251
24 10 10 00	1.00028107	23 09 29 00	1.00028393	25 09 29 00	1.00028720	23 00 00 00	1.00024193
24 10 45 00	1.00028117	23 10 35 00	1.00028423	25 10 30 00	1.00028710	23 00 45 00	1.00024356
24 12 10 00	1.00028077	23 11 30 00	1.00028423	25 11 35 00	1.00028700	23 01 00 00	1.00024296
24 14 10 00	1.00028097	23 12 40 00	1.00028413	25 12 29 00	1.00028751	23 02 00 00	1.00024397
24 14 45 00	1.00028127	23 17 40 00	1.00028469	25 13 30 00	1.00028761	23 02 45 00	1.00024354
25 02 10 00	1.00027927	23 18 34 00	1.00028429	25 14 25 00	1.00028843	23 03 00 00	1.00024388
25 02 52 00	1.00027927	23 19 30 00	1.00028429	25 15 30 00	1.00028690	23 04 00 00	1.00024494
25 04 10 00	1.00027927	23 20 40 00	1.00028128	25 16 17 00	1.00028495	23 04 45 00	1.00024494
25 06 10 00	1.00027998	23 21 33 00	1.00028157	25 17 15 00	1.00028406	23 05 00 00	1.00024453
25 06 46 00	1.00028019	23 22 30 00	1.00028205	25 18 16 00	1.00028198	23 06 00 00	1.00024458
25 08 10 00	1.00028099	23 23 26 00	1.00028137	25 19 24 00	1.00028043	23 06 49 00	1.00024432
25 10 10 00	1.00027999	24 00 30 00	1.00028452	25 20 20 00	1.00027929	23 07 00 00	1.00024414
25 10 45 00	1.00027999	24 01 40 00	1.00028679	25 21 24 00	1.00027929	23 08 00 00	1.00024357
25 12 10 00	1.00028099	24 02 40 00	1.00028710	25 22 20 00	1.00027812	23 08 40 00	1.00024295
25 14 10 00	1.00028067	24 03 50 00	1.00028699	25 23 26 00	1.00027966	23 08 45 00	1.00024278
25 14 22 00	1.00028119	24 04 35 00	1.00028710	26 00 20 00	1.00028084	23 09 00 00	1.00024269
25 16 10 00	1.00027770	24 05 40 00	1.00028750			23 10 00 00	1.00024548
		24 06 20 00	1.00028750	Santiago		23 11 09 00	1.00024522
Niguel		24 07 35 00	1.00028760			23 12 00 00	1.00024534
		24 08 35 00	1.00028811	22 09 00 00	1.00024098	23 12 45 00	1.00024566
22 09 28 00	1.00028344	24 09 30 00	1.00028713	22 10 00 00	1.00024157	23 19 30 00	1.00024599
22 10 32 00	1.00028413	24 10 30 00	1.00028835	22 10 40 00	1.00024174	23 20 00 00	1.00024581
22 11 30 00	1.00028463	24 11 39 00	1.00028906	22 10 46 00	1.00024166	23 21 00 00	1.00024514
22 12 30 00	1.00028523	24 12 31 00	1.00028917	22 11 00 00	1.00023980	23 22 00 00	1.00024629
22 13 31 00	1.00028513	24 13 33 00	1.00028927	22 12 00 00	1.00024139	23 23 00 00	1.00024808
22 14 30 00	1.00028286	24 14 31 00	1.00028958	22 12 42 00	1.00024140	24 00 00 00	1.00024900
22 15 41 00	1.00028362	24 15 35 00	1.00028793	22 12 46 00	1.00024157	24 01 45 00	1.00024917
22 16 36 00	1.00028224	24 16 17 00	1.00028693	22 12 50 00	1.00024157	24 02 45 00	1.00024917
22 17 30 00	1.00028107	24 17 20 00	1.00028392	22 13 00 00	1.00024183	24 03 45 00	1.00024949
22 18 31 00	1.00028020	24 18 17 00	1.00028402	22 14 00 00	1.00024200	24 04 45 00	1.00024967

Table A3. (continued)

Time dy hr mn sc	n	Time dy hr mn sc	n	Time dy hr mn sc	n	Time dy hr mn sc	n
24 05 45 00	1.00024949	25 02 43 00	1.00024679	26 00 20 00	1.00024337	24 04 45 00	1.00028056
24 06 25 00	1.00024940	25 02 51 00	1.00024670			24 05 00 00	1.00028056
24 06 40 00	1.00024931	25 03 00 00	1.00024679	San Juan		24 06 30 00	1.00028105
24 07 40 00	1.00024944	25 03 15 00	1.00024733			24 06 37 00	1.00028166
24 08 20 00	1.00024935	25 03 27 00	1.00024751	22 08 00 00	1.00027271	24 08 28 00	1.00028945
24 09 20 00	1.00024962	25 04 15 00	1.00024787	22 09 03 00	1.00027290	24 10 05 00	1.00027979
24 10 20 00	1.00024907	25 04 25 00	1.00024796	22 10 02 00	1.00027338	24 11 01 00	1.00028379
24 11 20 00	1.00024943	25 05 15 00	1.00024842	22 10 58 00	1.00027385	24 12 [illegible] 00	1.00028979
24 12 20 00	1.00024907	25 05 25 00	1.00024815	22 11 58 00	1.00027271	24 13 10 00	1.00028379
24 13 20 00	1.00024907	25 06 15 00	1.00024724	22 12 59 00	1.00027224	24 14 00 00	1.00028097
24 14 20 00	1.00024816	25 06 23 00	1.00024697	22 14 26 00	1.00027290	24 15 02 00	1.00028148
24 15 20 00	1.00024690	25 06 26 00	1.00024706	22 15 03 00	1.00027302	24 16 03 00	1.00028079
24 16 20 00	1.00024780	25 06 35 00	1.00024715	22 16 05 00	1.00027376	24 16 33 00	1.00028319
24 17 20 00	1.00024692	25 06 37 00	1.00024715	22 17 02 00	1.00027347	24 17 31 00	1.00027733
24 18 20 00	1.00024700	25 06 50 00	1.00024697	22 18 00 00	1.00027020	24 18 29 00	1.00027538
24 18 37 00	1.00024665	25 07 15 00	1.00024679	22 19 00 00	1.00026450	24 19 34 00	1.00027339
24 19 20 00	1.00024513	25 07 25 00	1.00024607	22 20 02 00	1.00026729	24 20 30 00	1.00027168
24 20 00 00	1.00024495	25 08 15 00	1.00024805	22 21 00 00	1.00026873	24 21 36 00	1.00027262
24 20 15 00	1.00024417	25 08 20 00	1.00024841	22 22 00 00	1.00027011	24 22 30 00	1.00027188
24 20 30 00	1.00024316	25 08 24 00	1.00024850	22 23 00 00	1.00027084	24 23 30 00	1.00027330
24 20 40 00	1.00024298	25 09 20 00	1.00024727	23 00 00 00	1.00027366	25 00 30 00	1.00027569
24 20 50 00	1.00024281	25 10 15 00	1.00024655	23 01 00 00	1.00027482	25 01 33 00	1.00027813
24 21 00 00	1.00024169	25 10 20 00	1.00024664	23 02 00 00	1.00027654	25 02 36 00	1.00027912
24 21 05 00	1.00024253	25 10 23 00	1.00024664	23 03 00 00	1.00027782	25 03 30 00	1.00027961
24 21 15 00	1.00024219	25 10 35 00	1.00024682	23 04 10 00	1.00027685	25 04 35 00	1.00027912
24 22 00 00	1.00024150	25 10 38 00	1.00024673	23 05 00 00	1.00027733	25 05 39 00	1.00027813
24 22 15 00	1.00024133	25 10 50 00	1.00024664	23 06 00 00	1.00027751	25 06 35 00	1.00027942
24 22 20 00	1.00024142	25 11 15 00	1.00024638	23 07 00 00	1.00027703	25 07 30 00	1.00027983
24 22 23 00	1.00024090	25 11 20 00	1.00024638	23 08 02 00	1.00027627	25 08 32 00	1.00027903
24 22 32 00	1.00024228	25 12 15 00	1.00024726	23 09 00 00	1.00027596	25 09 30 00	1.00027773
24 22 35 00	1.00024253	25 12 20 00	1.00024772	23 10 00 00	1.00027773	25 10 31 00	1.00027675
24 22 45 00	1.00024305	25 12 23 00	1.00024762	23 10 56 00	1.00027751	25 11 30 00	1.00027921
24 23 15 00	1.00024436	25 13 15 00	1.00024772	23 12 03 00	1.00027703	25 12 31 00	1.00027921
24 23 35 00	1.00024471	25 13 20 00	1.00024782	23 18 00 00	1.00027663	25 13 35 00	1.00028002
25 00 15 00	1.00024502	25 14 20 00	1.00024854	23 19 00 00	1.00027376	25 14 29 00	1.00028002
25 00 20 00	1.00024560	25 15 20 00	1.00024687	23 20 05 00	1.00027349	25 15 32 00	1.00027802
25 00 25 00	1.00024578	25 16 20 00	1.00024439	23 21 00 00	1.00027588	25 16 32 00	1.00027666
25 00 29 00	1.00024537	25 17 20 00	1.00024396	23 22 10 00	1.00027414	25 17 33 00	1.00027094
25 01 15 00	1.00024635	25 18 20 00	1.00024335	23 23 05 00	1.00027654	25 18 33 00	1.00027309
25 01 20 00	1.00024644	25 19 20 00	1.00024178	24 00 00 00	1.00027733	25 19 30 00	1.00027176
25 02 15 00	1.00024670	25 20 20 00	1.00024095	24 01 00 00	1.00027733	25 20 35 00	1.00026914
25 02 27 00	1.00024679	25 21 20 00	1.00024001	24 02 00 00	1.00027957	25 21 45 09	1.00026842
25 02 32 00	1.00024662	25 22 20 00	1.00024052	24 03 00 00	1.00028006	25 22 33 00	1.00026704
25 02 39 00	1.00024679	25 23 20 00	1.00024224	24 04 00 00	1.00028006	26 00 35 00	1.00027054

Table A4. Time-of-Flight Ratios

Castro					San Pedro					Niguel					Santiago					San Juan				
dy	hr	mn	sc	1.104+	dy	hr	mn	sc	0.948+	dy	hr	mn	sc	1.364+	dy	hr	mn	sc	1.210+	dy	hr	mn	sc	0.735+
22	10	04	29	914198	22	10	18	55	870439	24	04	20	32	486752	22	10	41	41	567622	22	10	51	17	646826
22	12	02	41	915170	22	12	21	52	871345	24	06	19	58	487793	22	12	43	11	567332	22	12	51	51	646994
22	14	05	43	914546	22	14	15	03	870661	24	06	46	28	485966	22	14	34	32	566961	22	14	48	04	647619
23	00	09	40	913745	22	18	23	39	871637	24	08	18	26	486255	22	22	49	55	566262	22	18	55	03	649189
23	02	09	25	913337	24	04	20	40	870474	24	10	15	13	486647	23	00	41	06	566832	22	22	54	50	648337
23	06	05	03	913747	24	06	16	19	871245	24	10	40	16	486057	23	04	33	04	566222	23	06	47	01	647875
24	06	08	46	914336	24	06	51	04	870690	24	14	15	10	486632	23	06	39	34	565878	23	08	47	14	647283
24	06	58	17	914200	24	08	09	40	871172	24	14	40	18	486914	23	08	39	44	565151	24	04	43	14	648393
24	08	00	19	913737	24	10	10	03	870674	24	16	18	20	486108	24	04	40	08	566802	24	05	29	45	647595
24	09	59	54	914011	24	10	45	34	870708	25	02	21	58	486409	24	06	25	43	566603	24	06	36	37	649039
24	10	55	03	914255	24	12	10	04	870911	25	02	48	49	485806	24	06	41	31	565969	24	08	25	49	648657
24	12	00	58	914457	24	14	11	30	870981	25	10	16	05	486836	24	08	22	17	566526	24	12	25	08	648343
24	14	01	34	914142	24	14	45	60	870330	25	10	41	13	486512	24	10	21	13	566338	24	14	25	20	649772
24	14	55	05	915268	25	02	13	18	870356						24	10	35	15	566618	24	14	38	04	649358
24	16	01	03	915165	25	02	53	27	871173						24	12	20	03	566316	24	16	22	54	649338
24	18	00	06	914538	25	04	09	53	869977						24	14	20	03	564893	25	02	33	03	648673
24	18	57	39	914327	25	06	10	05	870052						24	14	35	11	564750	25	02	36	56	648634
24	22	44	42	913891	25	06	45	43	870209						24	16	29	53	565410	25	04	25	60	650026
25	02	05	25	914683	25	08	11	36	871274						24	20	18	04	565626	25	06	32	42	648312
25	02	58	04	914826	25	10	10	16	871390						25	00	25	13	565089	25	08	23	56	647659
25	04	00	52	913710	25	10	45	23	870584						25	02	29	30	565803	25	10	25	11	647534
25	06	01	17	914789	25	12	10	30	871738						25	02	39	51	565623	25	10	30	03	647275
25	06	55	21	915255	25	14	15	11	871417						25	04	22	37	566544	25	12	25	03	648233
25	08	04	49	914402	25	14	40	42	871316						25	06	22	51	566702	25	18	31	55	647344
25	10	01	53	914614											25	06	35	48	566195	25	20	25	59	648656
25	10	55	08	915208											25	08	20	32	566493	25	22	28	58	646712
25	12	04	05	914277											25	10	20	08	566462	26	00	32	50	648933
25	14	51	54	915409											25	10	35	11	566062					
25	16	00	28	914909											25	12	21	02	565658					
25	18	00	19	914473											25	14	21	41	566251					
25	18	59	43	914613											25	14	35	02	566204					
25	20	07	42	914243											25	16	20	06	567037					
25	20	37	24	913952											25	18	39	42	566858					
25	20	49	58	914766											25	20	20	59	566413					
25	22	51	57	912786											25	22	37	54	565985					
26	00	05	27	912961											26	00	26	53	565337					

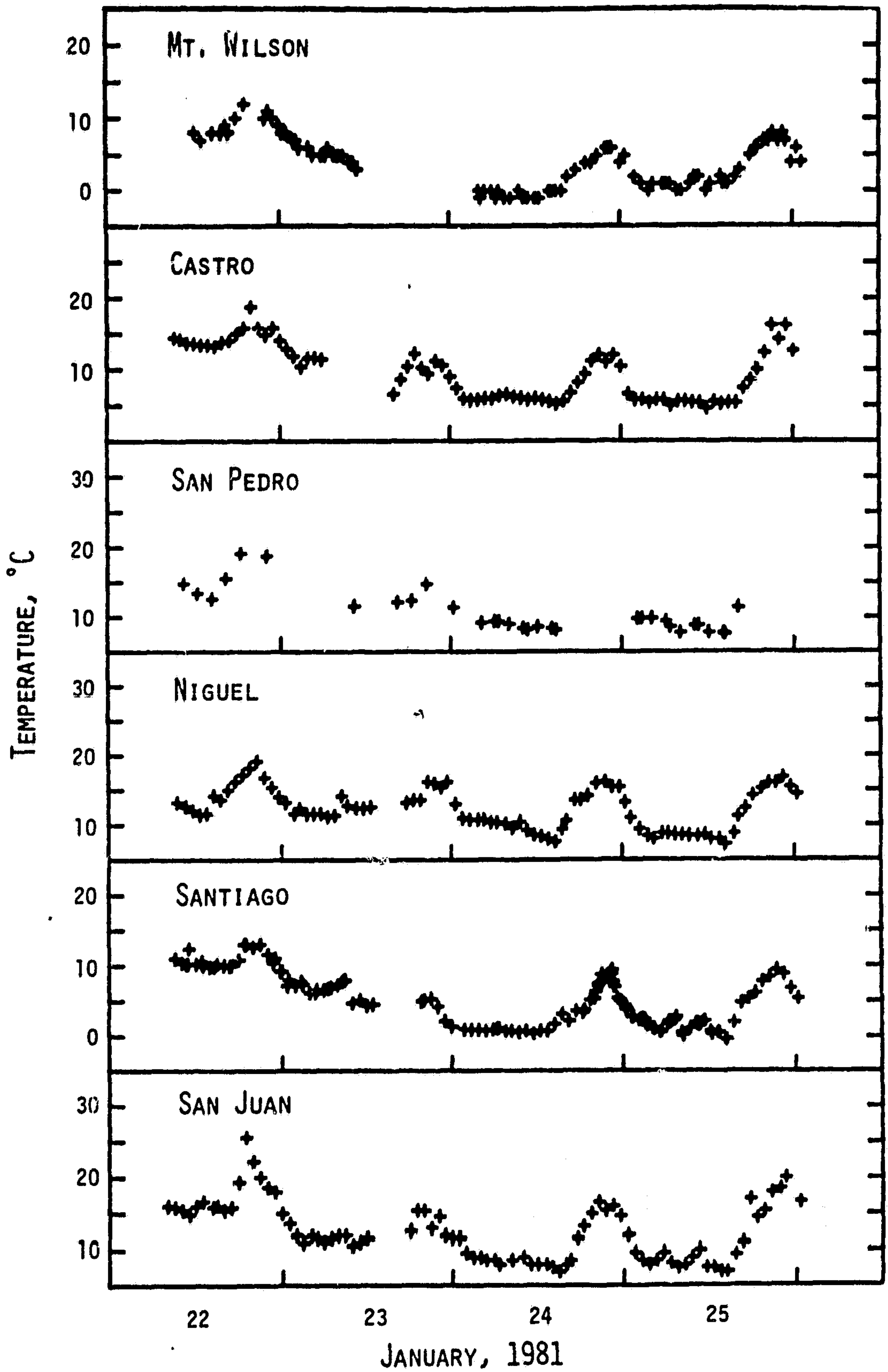

Fig. A1. Observed atmospheric temperature.

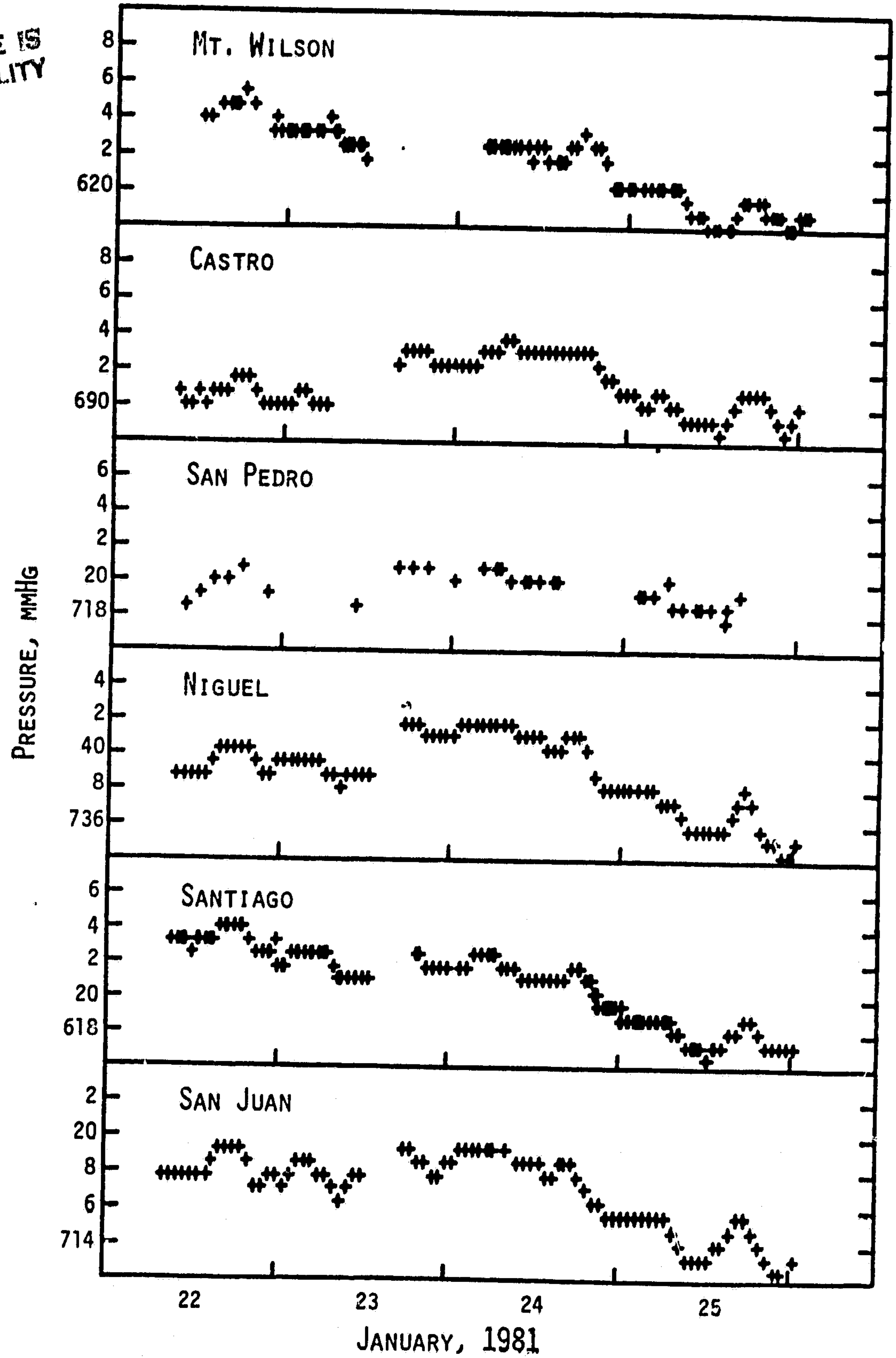

Fig. A2. Observed atmospheric pressure.

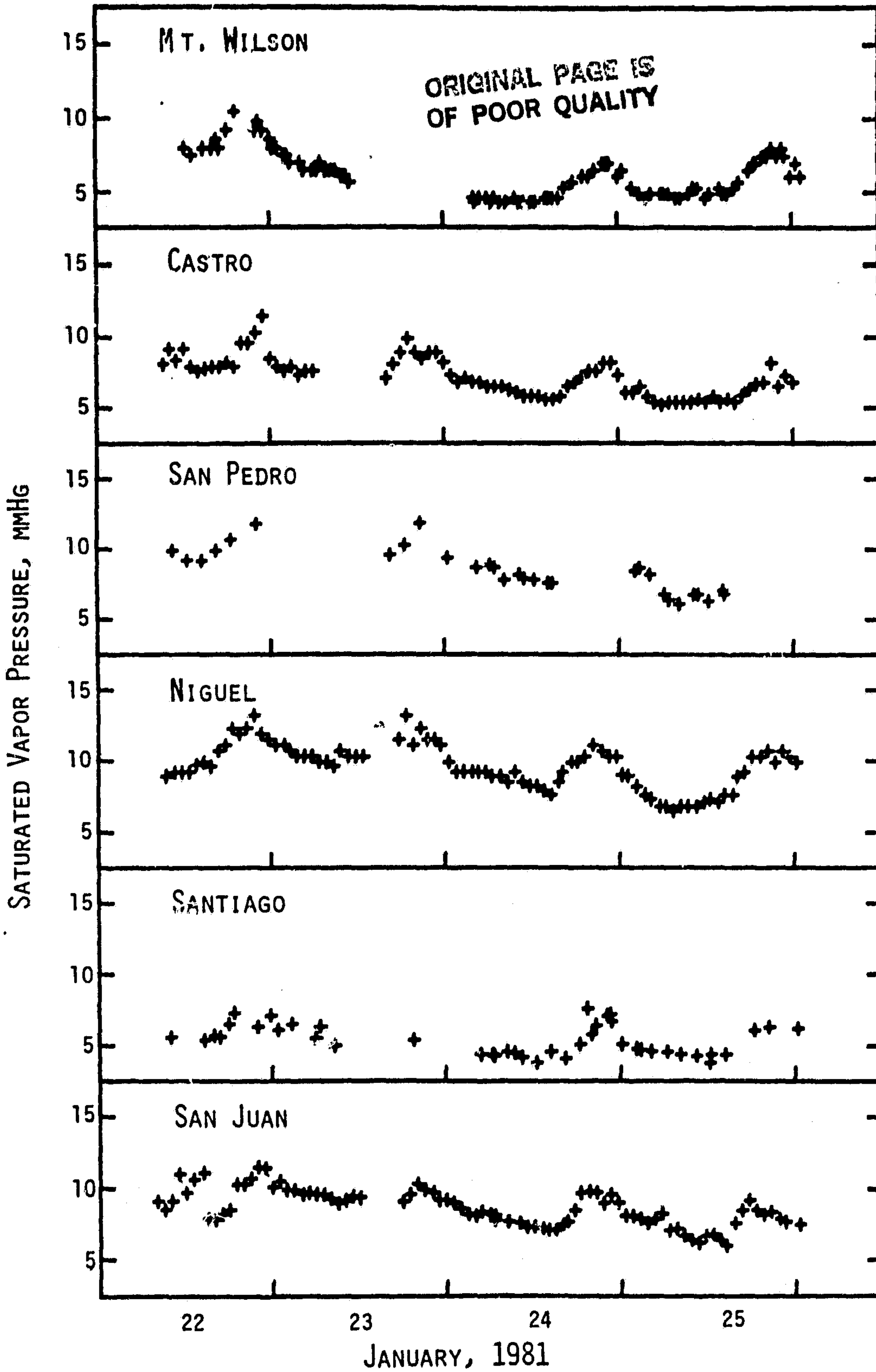

Fig. A3. Saturated vapor pressure.